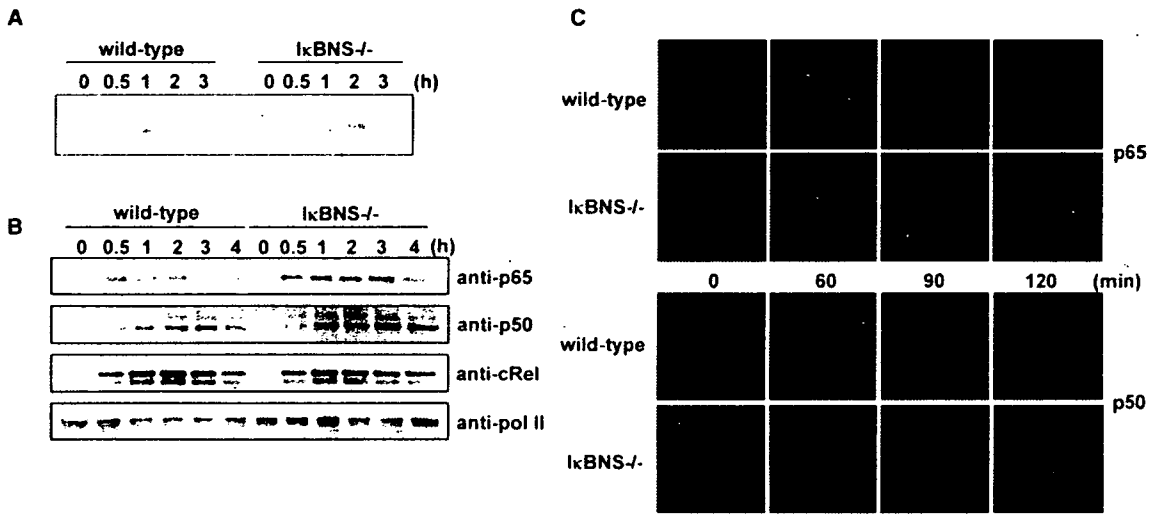

Figure 4. Persistent LPS-Induced Activation of NF-κB in IκBNS$^{-/-}$ Macrophages

(A) Peritoneal macrophages from wild-type and IκBNS$^{-/-}$ mice were stimulated with 100 ng/ml LPS. At the indicated time points, nuclear extracts were prepared, and NF-κB activation was analyzed by EMSA using a NF-κB specific probe.

(B) Peritoneal macrophages were stimulated with LPS. At the indicated time points, nuclear fractions were isolated and subjected to Western blotting using anti-p65 Ab, anti-p50 Ab, anti-cRel Ab, or anti-polII Ab.

(C) Macrophages were stimulated with LPS for the indicated periods. Then, cells were stained with anti-p65 Ab or anti-p50 Ab (red) as well as DAPI (blue), and analyzed by confocal microscopy. Merged images are shown.

IκBNS$^{-/-}$ cells. We next analyzed nuclear localization of NF-κB subunits. Peritoneal macrophages were stimulated with LPS for the indicated periods, and nuclear fractions were analyzed for expression of p65, p50, and c-Rel by immunoblotting (Figure 4B). In wild-type macrophages, nuclear translocation of p65 was observed within 30 min of LPS stimulation, and nuclear localized p65 gradually decreased thereafter. In contrast, nuclear localized p65 was still significantly observed even at 3 hr of LPS stimulation in IκBNS$^{-/-}$ cells. In addition, sustained nuclear localization of p50, but not c-Rel, was observed in IκBNS$^{-/-}$ macrophages (Figure 4B). Nuclear localization of NF-κB subunits was also analyzed by immunofluorescent staining of macrophages (Figure 4C). Without stimulation, p65 and p50 were localized in the cytoplasm, but not in the nucleus, in both wild-type and IκBNS$^{-/-}$ macrophages. LPS stimulation resulted in nuclear staining of both p65 and p50 at 1 hr. Nuclear staining of p65 and p50 gradually decreased after 1 hr of LPS stimulation and was only faintly observed at 2 hr of stimulation in wild-type cells. However, nuclear localization of p65 and p50 was still evident at 2 hr of LPS stimulation in IκBNS$^{-/-}$ cells. These findings indicate that LPS-induced NF-κB activity was prolonged in IκBNS$^{-/-}$ macrophages. NF-κB activity is terminated by degradation of promoter-bound p65 (Natoli et al., 2005; Saccani et al., 2004). We used RAW264.7 macrophage cell line and performed pulse-chase experiments with ^{35}S-labeled amino acids to analyze p65 turnover (Figure S3C). In these cells, labeled p65 was accumulated into the nucleus until 2 hr of LPS stimulation, and then p65 was degraded. In RAW cells constitutively expressing IκBNS, nuclear accumulation of labeled p65 was similarly observed until 1 hr of LPS stimulation. However, the p65 turnover was observed more rapidly and labeled p65 disappeared at 2 hr after LPS stimulation (Figure S3C). These findings indicate that IκBNS mediates the degradation of p65. The MyD88-dependent pathway mediates activation of MAP kinase cascades as well as NF-κB activation. Therefore, LPS-induced phosphorylation of p38, ERK1, ERK2, and JNK was analyzed by Western blotting (Figure S3D). LPS-induced activation of these MAP kinases was not compromised in IκBNS$^{-/-}$ macrophages.

Regulation of p65 Activity at the IL-6 Promoter by IκBNS

We next addressed how IκBNS selectively downregulates induction of genes that are induced late. We utilized the IL-6 and TNF-α promoters, which are representatives of genes activated late and early, respectively. Wild-type macrophages were stimulated with LPS and analyzed for recruitment of endogenous IκBNS to the promoters by chromatin immunoprecipitation (ChIP) assay (Figure 5A). Consistent with previous findings using IκBNS overexpressing macrophage cell lines (Hirotani et al., 2005), endogenous IκBNS was recruited to the IL-6 promoter, but not the TNF-α promoter, in LPS-stimulated macrophages. We next addressed LPS-induced recruitment of p65 to the promoters in wild-type and IκBNS$^{-/-}$ macrophages (Figure 5B). Recruitment of p65 to the TNF-α promoter peaked at 1 hr of LPS stimulation and gradually decreased thereafter in a similar manner in both wild-type and IκBNS$^{-/-}$ cells. Recruitment of p65 to the IL-6 promoter was observed to similar extents until 3 hr of LPS stimulation in wild-type and IκBNS$^{-/-}$ macrophages. After that, it decreased in wild-type macrophages. In contrast, p65 recruitment was still evident, rather enhanced, even after 5 hr of LPS stimulation in IκBNS$^{-/-}$ macrophages. Thus, p65 activity at

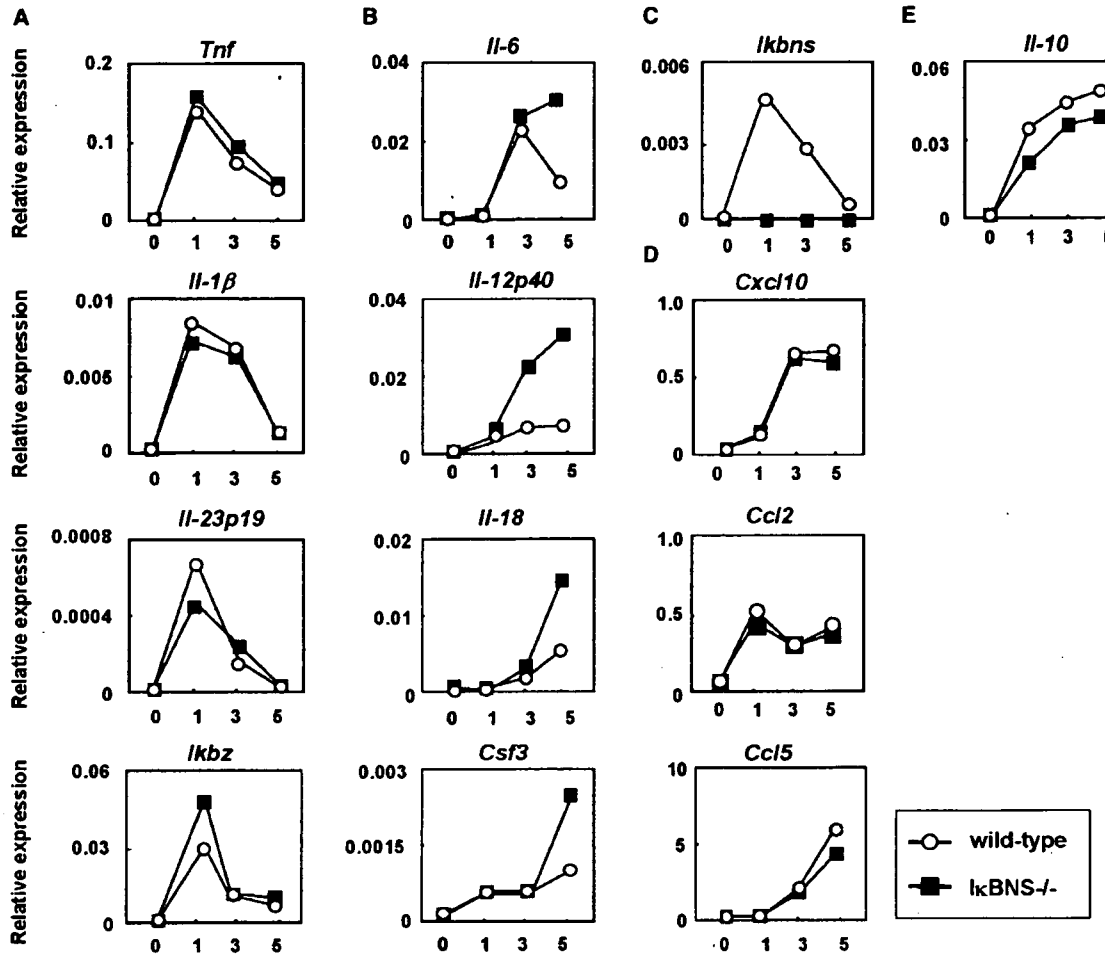

Figure 3. LPS-Induced Expression of Several TLR-Dependent Genes in IκBNS$^{-/-}$ Macrophages

Peritoneal macrophages from wild-type and IκBNS$^{-/-}$ mice were stimulated with 100 ng/ml LPS for the indicated periods. Total RNA was extracted, and then subjected to quantitative real-time RT-PCR analysis using primers specific for *Tnf*, *Il-1β*, *Il-23p19*, *Ikbz* (A), *Il-6*, *Il-12p40*, *Il-18*, *Csf3* (B), *Ikbns* (C), *Cxcl10*, *Ccl2*, *Ccl5* (D), and *Il-10* (E). The fold difference of each sample relative to EF-1α levels is shown. Representative of three independent experiments.

IκBNS$^{-/-}$ cells. We also analyzed LPS-induced expression of *Cxcl10* (IP-10), *Ccl2* (MCP-1), and *Ccl5* (RANTES), which are induced by the TRIF-dependent activation of IRF-3 (Figure 3D). LPS-induced expression of these genes was not altered in IκBNS$^{-/-}$ macrophages. An anti-inflammatory cytokine IL-10 is induced by TLR stimulation and thereby inhibits TLR-dependent gene induction (Moore et al., 2001). Therefore, we next addressed LPS-induced IL-10 mRNA expression (Figure 3E). LPS-induced IL-10 mRNA expression was comparable between wild-type and IκBNS$^{-/-}$ macrophages. In addition, LPS-induced production of IL-10 protein was not compromised in IκBNS$^{-/-}$ DCs (Figure S2C). These findings indicate that the enhanced LPS-induced expression of a subset of TLR-dependent genes was not due to the impaired IL-10 production in IκBNS$^{-/-}$ mice.

Prolonged NF-κB Activity in IκBNS-Deficient Cells

Gene expression of *Cxcl10* (IP-10), *Ccl2* (MCP-1), and *Ccl5* (RANTES) was mainly regulated by the transcription factor IRF-3 in the TRIF-dependent pathway, whereas TNF-α, IL-6, and IL-12p40 gene expression was mainly regulated by the MyD88-dependent activation of NF-κB (Akira and Takeda, 2004; Yamamoto et al., 2003). In addition, previous in vitro studies indicated that overexpression of IκBNS leads to compromised NF-κB activity through selective association of IκBNS with p50 subunit of NF-κB (Fiorini et al., 2002; Hirotani et al., 2005). Therefore, we next analyzed LPS-induced activation of NF-κB. LPS-induced degradation of IκBα was not compromised in IκBNS$^{-/-}$ macrophages (Figure S3A). Next, peritoneal macrophages or bone marrow-derived macrophages were stimulated with LPS and DNA binding activity was analyzed by EMSA (Figure 4A; Figure S3B). LPS stimulation resulted in enhanced DNA binding activity of NF-κB in both wild-type and IκBNS$^{-/-}$ macrophages to similar extents within 1 hr. After 1 hr of LPS stimulation, NF-κB activity decreased in wild-type cells. However, NF-κB activity sustained and even at 3 hr of LPS stimulation significant DNA binding activity was still observed in

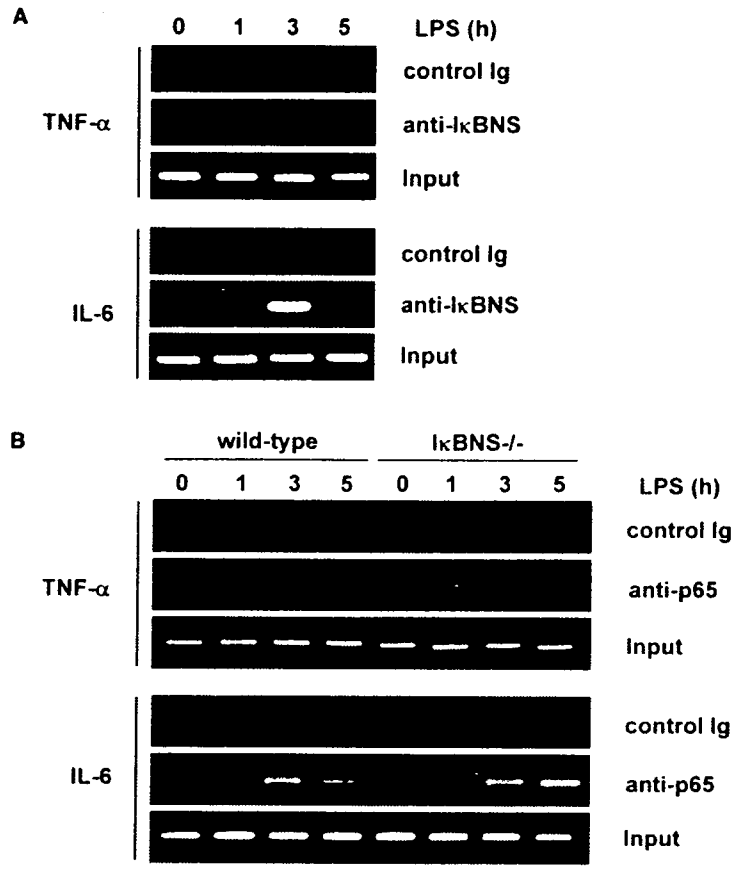

Figure 5. IκBNS Regulation of p65 Activity at the IL-6 Promoter

(A) Wild-type bone marrow-derived macrophages were stimulated with 100 ng/ml of LPS for the indicated periods, and chromatin immunoprecipitation (ChIP) assay was performed with anti-IκBNS Ab or control Ig. The immunoprecipitated TNF-α promoter (upper panel) or IL-6 promoter (lower panel) was analyzed by PCR with promoter-specific primers. PCR amplification of the total input DNA in each sample is shown (Input). Representative of three independent experiments. The same result was obtained when peritoneal macrophages were used.

(B) Macrophages from wild-type or IκBNS$^{-/-}$ mice were stimulated with LPS for the indicated periods. Then, ChIP assay was performed with anti-p65 Ab or control Ig. The immunoprecipitated TNF-α promoter (upper panel) or IL-6 promoter (lower panel) was analyzed by PCR with promoter-specific primers. Representative of three independent experiments.

the IL-6 promoter, but not at the TNF-α promoter, was prolonged in LPS-stimulated IκBNS$^{-/-}$ macrophages. Taken together, these findings indicate that TLR-inducible IκBNS is responsible for termination of NF-κB activity through its recruitment to specific promoters.

High Sensitivity to LPS-Induced Endotoxin Shock in IκBNS-Deficient Mice

To study the in vivo role of IκBNS, we examined LPS-induced endotoxin shock. Intraperitoneal injection of LPS resulted in marked increases in serum concentrations of TNF-α, IL-6, and IL-12p40 (Figure 6A). TNF-α level was comparable between wild-type and IκBNS$^{-/-}$ mice, which rapidly peaked at around 1.5 hr of LPS administration. In the case of IL-6 and IL-12p40 levels, concentrations of both cytokines were almost equally elevated within 3 hr of LPS injection. After 3 hr, levels of both cytokines gradually decreased in wild-type mice. However, concentrations of IL-6 and IL-12p40 sustained, rather enhanced, in IκBNS$^{-/-}$ mice after 3 hr. Thus, persistently high concentrations of LPS-induced serum IL-6 and IL-12p40 were observed in IκBNS$^{-/-}$ mice. Furthermore, high sensitivity to LPS-induced lethality was observed in IκBNS$^{-/-}$ mice (Figure 6B). All IκBNS$^{-/-}$ mice died within 4 days of LPS challenge at a dose of which almost all wild-type mice survived over 4 days. These findings indicate that IκBNS$^{-/-}$ mice are highly sensitive to LPS-induced endotoxin shock.

High Susceptibility to DSS-Induced Colitis in IκBNS$^{-/-}$ Mice

In a previous report, IκBNS was shown to be constitutively expressed in macrophages residing in the colonic lamina propria, which explains one of the mechanisms for hyporesponsiveness to TLR stimulation in these cells (Hirotani et al., 2005). Therefore, we next stimulated CD11b^{+} cells isolated from the colonic lamina propria with LPS and analyzed for production of TNF-α and IL-6 (Figure S4). In CD11b^{+} cells from wild-type mice, LPS-induced production of these cytokines was not significantly observed. In cells from IκBNS$^{-/-}$ mice, IL-6 production was increased even in the absence of stimulation, and LPS stimulation led to markedly enhanced production of IL-6, but not TNF-α. In the next experiment, in order to expose these cells to microflora and cause intestinal inflammation, mice were orally administered with dextran sodium sulfate (DSS), which is toxic to colonic epithelial cells and therefore disrupts the epithelial cell barrier (Kitajima et al., 1999). IκBNS$^{-/-}$ mice showed more severe weight loss compared with wild-type mice (Figure 7A). Histological analyses of the colon indicated that the inflammatory lesions were more severe and more extensive in IκBNS$^{-/-}$ mice (Figures 7B and 7C). Thus, IκBNS$^{-/-}$ mice are highly susceptible to intestinal inflammation. Th1-oriented CD4^{+} T cell response was shown to be associated with DSS colitis (Strober et al., 2002). Therefore, we analyzed IFN-γ

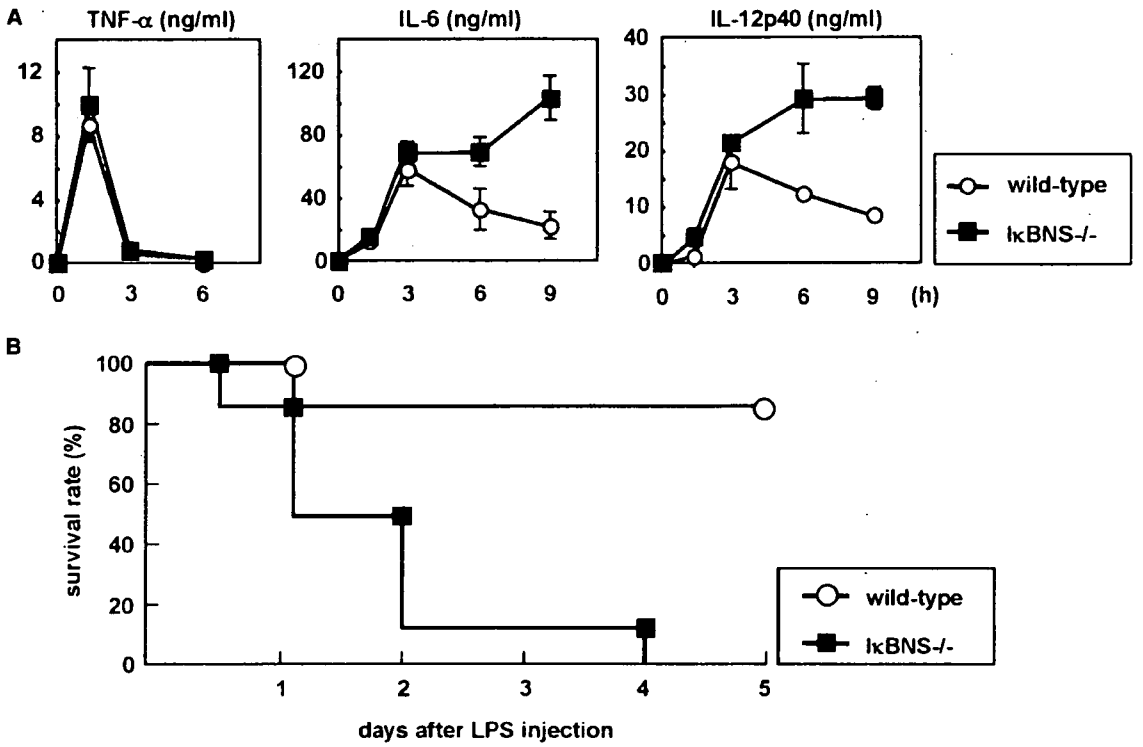

Figure 6. High Susceptibility to LPS-Induced Endotoxin Shock in IκBNS$^{-/-}$ Mice

Age-matched wild-type (n = 6) and IκBNS −/− (n = 6) mice were intraperitoneally injected with LPS (1 mg). (A) Sera were taken at 1.5, 3, 6, and 9 hr after LPS injection. Serum concentrations of TNF-α, IL-6, and IL-12p40 were determined by ELISA. Results are shown as mean ± SD of serum samples from six mice. (B) Survival was monitored for 5 days.

production from splenic CD4$^+$ T cells of wild-type and IκBNS$^{-/-}$ mice before and after DSS administration (Figure 7D). DSS administration led to a mild increase in IFN-γ production in wild-type mice. In nontreated IκBNS$^{-/-}$ mice, IFN-γ production was slightly increased compared with nontreated wild-type mice. In DSS-fed IκBNS$^{-/-}$ mice, a significant increase in IFN-γ production was observed compared to DSS-fed wild-type mice. These results indicate that IκBNS$^{-/-}$ mice are susceptible to intestinal inflammation caused by exposure to microflora.

Discussion

In the present study, we characterized the physiological function of IκBNS. Induced by TLR stimulation, IκBNS is involved in termination of NF-κB activity and thereby inhibits a subset of TLR-dependent genes that are induced late through MyD88-dependent NF-κB activation. Accordingly, IκBNS$^{-/-}$ mice show sustained production of IL-6 and IL-12p40, resulting in high susceptibility to LPS-induced endotoxin shock. Furthermore, IκBNS$^{-/-}$ mice are susceptible to intestinal inflammation accompanied by enhanced Th1 responses.

IκBNS was originally identified as a molecule that mediates negative selection of thymocytes (Fiorini et al., 2002). However, IκBNS$^{-/-}$ mice did not show any defect in T cell development. Requirement of IκBNS in negative selection of thymocytes should be analyzed precisely using peptide-specific TCR transgenic mice, such as mice bearing the H-Y TCR, in the future (Kisielow et al., 1988).

Recent studies have established that TLR-dependent gene induction is regulated mainly by NF-κB and IRF families of transcription factors (Akira and Takeda, 2004; Honda et al., 2005; Takaoka et al., 2005). In TLR4 signaling, the TRIF-dependent pathway is responsible for induction of IFN-β and IFN-inducible genes through activation of IRF-3, whereas the MyD88-dependent pathway mediates induction of several NF-κB dependent genes (Beutler, 2004). A study with mice lacking IκBζ, another member of nuclear IκB proteins, has demonstrated that the MyD88-dependent genes are divided into at least two types; one is induced early and independent of IκBζ, and another is induced late and dependent on IκBζ (Yamamoto et al., 2004). The IκBζ-regulated genes include IL-6, IL-12p40, IL-18, and G-CSF, which are all upregulated in LPS-stimulated IκBNS$^{-/-}$ macrophages. Thus, IκBNS seems to possess a function quite opposite to IκBζ. IκBNS is most structurally related to IκBζ (Fiorini et al., 2002; Hirotani et al., 2005). But, IκBζ has an additional N-terminal structure, which seemingly mediates the induction of target genes (Motoyama et al., 2005). Thus, nuclear IκB proteins IκBζ and IκBNS positively and negatively regulate a subset of TLR-induced NF-κB-dependent genes, respectively.

Recently, negative regulation of TLR-dependent gene induction was extensively analyzed (Liew et al., 2005).

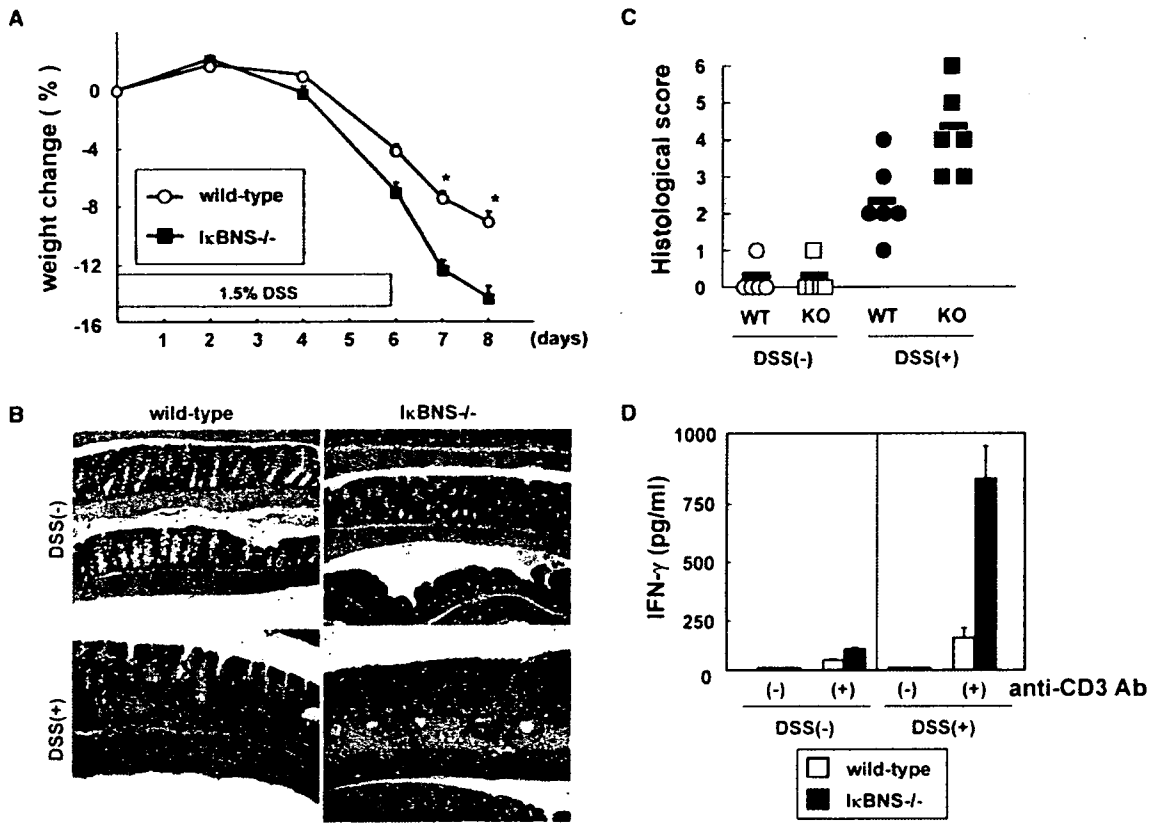

Figure 7. High Susceptibility to DSS Colitis in IκBNS$^{-/-}$ Mice

(A) Wild-type (n = 15) and IκBNS$^{-/-}$ mice (n = 15) were given 1.5% DSS in drinking water for 6 days and weighed everyday. Data are mean ± SD. *, $p < 0.05$.

(B) Histologic examination of the colons of wild-type and IκBNS$^{-/-}$ mice before or 9 days after initiation of DSS administration. H&E staining is shown. Representative of six mice examined. Magnification, 20×.

(C) The colitis scores shown for individual wild-type (circle) and IκBNS$^{-/-}$ mice (square) before (open) and after (closed) DSS treatment were total scores for individual sections as described in the Experimental Procedures section. Mean score for each group is also shown (black bar).

(D) CD4$^+$ T cells were purified from spleen of wild-type or IκBNS$^{-/-}$ mice either treated or nontreated with DSS. Then, CD4$^+$ T cells were cultured in the presence or absence of plate bound anti-CD3 Ab for 24 hr. Concentration of IFN-γ in the culture supernatants was measured by ELISA.

So far, characterized negative regulators are mainly involved in blockade of TLR signaling pathways in the cytoplasm or on the cell membrane. Accordingly, these negative regulators globally inhibit TLR-dependent gene induction. The nuclear IκB protein IκBNS is unique in that this molecule negatively regulates induction of a set of TLR-dependent genes by directly affecting NF-κB activity in the nucleus. Thus, TLR-dependent innate immune responses are regulated through a variety of mechanisms.

IκBNS-mediated inhibition of a set of TLR-dependent genes is probably explained by recruitment of IκBNS to the specific promoters. IκBNS was recruited to the IL-6 promoter, but not to the TNF-α promoter. In addition, LPS-induced recruitment of p65 to the TNF-α promoter was observed within 1 hr, whereas p65 recruitment to the IL-6 promoter was observed late, indicating that NF-κB activity was differentially regulated at both promoters. NF-κB activity at the TNF-α promoter is regulated in an IκBNS-independent manner, whereas the activity at the IL-6 promoter was IκBNS-dependent. Indeed, p65 recruitment to the TNF-α promoter was observed similarly in wild-type and IκBNS$^{-/-}$ macrophages, but the recruitment to the IL-6 promoter was sustained in IκBNS$^{-/-}$ cells. Previous reports indicate that IκBNS selectively associates with p50 subunit of NF-κB and affects NF-κB DNA binding activity (Fiorini et al., 2002; Hirotani et al., 2005). Consistent with these observations, IκBNS$^{-/-}$ macrophages showed prolonged LPS-induced NF-κB DNA binding activity and nuclear localization of p65. Taken together, these findings indicate that IκBNS, which is rapidly induced by TLR stimulation, might be recruited to gene promoters through association with p50, and contribute to termination of NF-κB activity. Termination of NF-κB activity has been shown to be induced by IKKα-mediated degradation of promoter-bound p65 (Lawrence et al., 2005). However, consistent with a recent report, we were not able to detect LPS-induced degradation of p65 in peritoneal macrophages and bone marrow-derived macrophages (Li et al., 2005). However, we could detect LPS-induced p65 degradation in the RAW264.7 macrophage cell line. In these cells, when constitutively expressed IκBNS, LPS-induced p65 turnover was

accelerated, indicating that IκBNS is involved in the degradation of promoter-bound p65. In the case of the TNF-α promoter, it is possible that NF-κB activity is already terminated when IκBNS expression is induced, and therefore IκBNS is no longer recruited to the TNF-α promoter. Alternatively, an unidentified mechanism that regulates selective recruitment of IκBNS to gene promoters might exist. The mechanisms by which IκBNS is recruited to the specific promoters through association with p50 remain unclear and would be a subject of further investigation.

Analyses of IκBNS$^{-/-}$ mice further highlighted the in vivo functions of IκBNS in limiting systemic and intestinal inflammation. IκBNS$^{-/-}$ mice succumbed to systemic LPS-induced endotoxin shock possibly due to sustained production of several TLR-dependent gene products such as IL-6 and IL-12p40. Furthermore, IκBNS$^{-/-}$ mice are more susceptible to intestinal inflammation induced by disruption of the epithelial barrier. Abnormal activation of innate immune cells caused by deficiency of IL-10 or Stat3 leads to spontaneous development of colonic inflammation (Kobayashi et al., 2003; Kuhn et al., 1993; Takeda et al., 1999). IκBNS$^{-/-}$ mice did not develop chronic colitis spontaneously until 20 week-old of age (our unpublished data). In Stat3 mutant mice, TLR-dependent production of proinflammatory cytokines increased over 10-fold compared to wild-type cells, which might contribute to the spontaneous intestinal inflammation (Takeda et al., 1999). In IκBNS$^{-/-}$ mice, increase in TLR-dependent production of proinflammatory cytokines such as IL-6 and IL-12p40 was mild compared to Stat3 mutant mice. In this case, the colonic epithelial barrier might contribute to prevention of excessive inflammatory responses in IκBNS$^{-/-}$ mice. However, when the barrier function of epithelial cells was disrupted by administration of DSS, IκBNS$^{-/-}$ mice suffered from severe intestinal inflammation accompanied by enhanced Th1 responses. IκBNS was shown to be expressed in CD11b^{+} cells residing in the colonic lamina propria (Hirotani et al., 2005). Therefore, in the absence of IκBNS, exposure of innate immune cells to intestinal microflora might result in increased or sustained production of proinflammatory cytokines such as IL-12p40, which induces exaggerated intestinal inflammation and Th1 cell development. Thus, IκBNS is responsible for the prevention of uncontrolled inflammatory responses in vivo.

In this study, we have shown that IκBNS is a selective inhibitor of TLR-dependent genes possibly through termination of NF-κB activity. Furthermore, IκBNS was responsible for prevention of inflammation through inhibition of persistent proinflammatory cytokine production. Future study that discloses the precise molecular mechanisms by which the nuclear IκB protein selectively inhibits TLR-dependent genes will provide basis for the development of new therapeutic strategies to a variety of inflammatory diseases.

Experimental Procedures

Generation of IκBNS-Deficient Mice

The *Ikbns* gene consists of eight exons (Figure 1A). The targeting vector was designed to replace a 1.8 kb fragment containing exons 5–8 of the *Ikbns* gene with a neomycin-resistance gene (*neo*). A short arm and a long arm of the homology region from the E14.1 ES genome were amplified by PCR. A herpes simplex virus thymidine kinase gene (HSV-TK) was inserted into the 3′ end of the vector. After the targeting vector was electroporated into ES cells, G418 and gancyclovir doubly resistant clones were selected and screened for homologous recombination by PCR and verified by Southern blot analysis using the probe indicated in Figure 1A. Two independently identified targeted ES clones were microinjected into C57BL/6 blastocysts. Chimeric mice were mated with C57BL/6 female mice, and heterozygous F1 progenies were intercrossed to obtain IκBNS$^{-/-}$ mice. Mice from these independent ES clones displayed identical phenotypes. All animal experiments were conducted according to guidelines of Animal Care and Use Committee at Kyushu University.

Reagents

LPS (*E. coli* 055:B5) was purchased from Sigma. Peptidoglycan was from Fluca. Pam_3CSK_4, MALP-2, and imiquimod were from Invivogen. Antibodies against p65 (C-20; sc-372), p50 (H-119; sc-7178 or NLS; sc-114), c-Rel (C; sc-71), and RNA polymerase II (H-224; sc-9001) were purchased from Santa Cruz. Rabbit anti-IκBNS Ab was generated against synthetic peptide (1-MEDSLDTRLY PEPSLSQVC-18) corresponding to N-terminal region of mouse IκBNS (MBL, Nagoya, Japan), and anti-IκBNS serum was affinity-purified using a column containing peptide-conjugated Sepharose 4B.

Preparation of Macrophages and Dendritic Cells

For isolation of peritoneal macrophages, mice were intraperitoneally injected with 2 ml of 4% thioglycollate medium (Sigma). Peritoneal exudate cells were isolated from the peritoneal cavity 3 days post injection. Cells were incubated for 2 hr and washed three times with HBSS. Remaining adherent cells were used as peritoneal macrophages for the experiments. To prepare bone marrow-derived macrophages, bone marrow cells were prepared from femora and tibia and passed through nylon mesh. Then cells were cultured in RPMI 1640 medium supplemented with 10% FCS, 100 μM 2-ME, and 10 ng/ml M-CSF (GenzymeTechne). After 6–8 days, the cells were used as macrophages for the experiments. Bone marrow-derived DCs were prepared by culturing bone marrow cells in RPMI 1640 medium supplemented with 10% FCS, 100 μM 2-ME, and 10 ng/ml GM-CSF (GenzymeTechne). After 6 days, the cells were used as DCs.

Measurement of Cytokine Production

Peritoneal macrophages or DCs were stimulated with various TLR ligands for 24 hr. Culture supernatants were collected and analyzed for TNF-α, IL-6, IL-12p40, IL-12p70, or IL-10 production with enzyme-linked immunosorbent assay (ELISA). Mice were intravenously injected with 1mg of LPS and bled at the indicated periods. Serum concentrations of TNF-α, IL-6, and IL-12p40 were determined by ELISA. ELISA kits were purchased from GenzymeTechne and R&D Systems. For measurement of IFN-γ, CD4^{+} T cells were purified from spleen cells using CD4 microbeads (Miltenyi Biotec) and stimulated by plate bound anti-CD3ε antibody (145-2C11, BD PharMingen) for 24 hr. Concentrations of IFN-γ in the supernatants were determined by ELISA (GenzymeTechne).

Quantitative Real-Time RT-PCR

Total RNA was isolated with TRIzol reagent (Invitrogen, Carlsbad, CA), and 2 μg of RNA was reverse transcribed using M-MLV reverse transcriptase (Promega, Madison, WI) and oligo (dT) primers (Toyobo, Osaka, Japan) after treatment with RQ1 DNase I (Promega). Quantitative real-time PCR was performed on an ABI 7700 (Applied Biosystems, Foster City, CA) using TaqMan Universal PCR Master Mix (Applied Biosystems). All data were normalized to the corresponding elongation factor-1α (EF-1α) expression, and the fold difference relative to the EF-1α level was shown. Amplification conditions were: 50°C (2 min), 95°C (10 min), 40 cycles of 95°C (15 s), and 60°C (60 s). Each experiment was performed independently at least three times, and the results of one representative experiment are shown. All primers were purchased from Assay on Demand (Applied Biosystems).

Electrophoretic Mobility Shift Assay

Macrophages were stimulated with 100 ng/ml LPS for the indicated periods. Then, nuclear proteins were extracted, and incubated with an end-labeled, double-stranded oligonucleotide containing an NF-κB binding site of the IL-6 promoter in 25 μl of binding buffer (10 mM HEPES-KOH, [pH 7.8], 50 mM KCl, 1 mM EDTA [pH 8.0], 5 mM $MgCl_2$ and 10% glycerol) for 20 min at room temperature and loaded on a native 5% polyacrylamide gel. The DNA-protein complexes were visualized by autoradiography.

Western Blotting

Cells were lysed with RIPA buffer (50 mM Tris-HCl [pH 7.5], 150 mM NaCl, 1% Triton X-100, 0.5% Na-deoxycholate) containing protease inhibitors (Complete Mini; Roche). The lysates were separated on SDS-PAGE and transferred to PVDF membrane. The membranes were incubated with anti-IκBα Ab, anti-ERK Ab, anti-p38 Ab, anti-JNK Ab (Santa Cruz Biotechnology), anti-phospho-p38 Ab, anti-phospho-ERK Ab, or anti-phospho-JNK Ab (Cell Signaling Technology). Bound Abs were detected with SuperSignal West Pico Chemiluminescent Substrate (Pierce).

Immunofluorescence Staining

Macrophages were stimulated with 100 ng/ml LPS for the indicated periods, washed with Tris-buffered saline (TBS), and fixed with 3.7% formaldehyde in TBS for 15 min at room temperature. After permeabilization with 0.2% Triton X-100, cells were washed with TBS and incubated with 10 ng/ml of a rabbit anti-p50 or anti-p65 Ab (Santa Cruz Biotechnology) in TBS containing 1% bovine serum albumin, followed by incubation with Alexa Fluor 594-conjugated goat anti-rabbit immunoglobulin G (IgG; Molecular Probes, Eugene, OR). To stain the nucleus, cells were cultured with 0.5 μg/ml 4, 6-diamidino-2-phenylindole (DAPI; Wako, Osaka, Japan). Stained cells were analyzed using an LSM510 model confocal microscope (Carl Zeiss, Oberkochem, Germany).

Chromatin Immunoprecipitation

Chromatin immunoprecipitation (ChIP) was performed essentially with a described protocol (Upstate Biotechnology, Lake Placid, NY). In brief, peritoneal macrophages from wild-type and $I\kappa BNS^{-/-}$ mice were stimulated with 100 ng/ml LPS for 1, 3, or 5 hr, and then fixed with formaldehyde for 10 min. The cells were lysed, sheared by sonication using Bioruptor (CosmoBio), and incubated overnight with specific antibody followed by incubation with protein A-agarose saturated with salmon sperm DNA (Upsate Biotechnology). Precipitated DNA was analyzed by quantitative PCR (35 cycles) using primers 5′- CCCCAGATTGCCACAGAATC -3′ and 5′- CCAGT GAGTGAAAGGGACAG -3′ for the TNF-α promoter and 5′- TGTGTG TCGTCTGTCATGCG-3′ and 5′- AGCTACAGACATCCCCAGTCTC -3′ for the IL-6 promoter.

Induction of DSS Colitis

Mice received 1.5% (wt/vol) DSS (40,000 kDa; ICN Biochemicals), ad libitum, in their drinking water for 6 days, then switched to regular drinking water. The amount of DSS water drank per animal was recorded and no differences in intake between strains were observed. Mice were weighed for the determination of percent weight change. This was calculated as: percentage weight change = (weight at day X-day 0/weight at day 0) × 100. Statistical significance was determined by paired Student's t test. Differences were considered to be statistically significant at $p < 0.05$.

Histological Analysis

Colon tissues were fixed in 4% paraformaldehyde, rolled up, and embedded in paraffin in a Swiss roll orientation such that the entire length of the intestinal tract could be identified on single sections. After sectioning, the tissues were dewaxed in ethanol, rehydrated, and stained hematoxylin and eosin to study histological changes after DSS-induced damage. Histological scoring was performed in a blinded fashion by a pathologist, with a combined score for inflammatory cell infiltration (score, 0–3) and tissue damage (score, 0–3) (Araki et al., 2005). The presence of occasional inflammatory cells in the lamina propria was assigned a value of 0; increased numbers of inflammatory cells in the lamina propria as 1; confluence of inflammatory cells, extending into the submucosa, as 2; and transmural extension of the infiltrate as 3. For tissue damage, no mucosal damage was scored as 0; discrete lymphoepithelial lesions were scored as 1; surface mucosal erosion or focal ulceration was scored as 2; and extensive mucosal damage and extension into deeper structures of the bowel wall were scored as 3. The combined histological score ranged from 0 (no changes) to 6 (extensive cell infiltration and tissue damage).

Supplemental Data

Supplemental Data include four figures and are available with this article online at http://www.immunity.com/cgi/content/full/24/1/41/DC1/.

Acknowledgments

We thank Y. Yamada, K. Takeda, M. Otsu, and N. Kinoshita for technical assistance; M. Yamamoto and S. Akira for providing us with reagents, P. Lee for critical reading of the manuscript, and M. Kurata for secretarial assistance. This work was supported by grants from the Special Coordination Funds of the Ministry of Education, Culture, Sports, Science and Technology; the Uehara Memorial Foundation; the Mitsubishi Foundation; the Takeda Science Foundation; the Tokyo Biochemical Research Foundation; the Kowa Life Science Foundation; the Osaka Foundation for Promotion of Clinical Immunology; and the Sankyo Foundation of Life Science.

Received: July 15, 2005
Revised: September 16, 2005
Accepted: November 16, 2005
Published: January 17, 2006

References

Akira, S., and Takeda, K. (2004). Toll-like receptor signalling. Nat. Rev. Immunol. *4*, 499–511.

Araki, A., Kanai, T., Ishikura, T., Makita, S., Uraushihara, K., Iiyama, R., Totsuka, T., Takeda, K., Akira, S., and Watanabe, M. (2005). MyD88-deficient mice develop severe intestinal inflammation in dextran sodium sulfate colitis. J. Gastroenterol. *40*, 16–23.

Beutler, B. (2004). Inferences, questions and possibilities in Toll-like receptor signalling. Nature *430*, 257–263.

Bjorkbacka, H., Kunjathoor, V.V., Moore, K.J., Koehn, S., Ordija, C.M., Lee, M.A., Means, T., Halmen, K., Luster, A.D., Golenbock, D.T., and Freeman, M.W. (2004). Reduced atherosclerosis in MyD88-null mice links elevated serum cholesterol levels to activation of innate immunity signaling pathways. Nat. Med. *10*, 416–421.

Boone, D.L., Turer, E.E., Lee, E.G., Ahmad, R.C., Wheeler, M.T., Tsui, C., Hurley, P., Chien, M., Chai, S., Hitotsumatsu, O., et al. (2004). The ubiquitin-modifying enzyme A20 is required for termination of Toll-like receptor responses. Nat. Immunol. *5*, 1052–1060.

Brint, E.K., Xu, D., Liu, H., Dunne, A., McKenzie, A.N., O'Neill, L.A., and Liew, F.Y. (2004). ST2 is an inhibitor of interleukin 1 receptor and Toll-like receptor 4 signaling and maintains endotoxin tolerance. Nat. Immunol. *5*, 373–379.

Burns, K., Janssens, S., Brissoni, B., Olivos, N., Beyaert, R., and Tschopp, J. (2003). Inhibition of interleukin 1 receptor/Toll-like receptor signaling through the alternatively spliced, short form of MyD88 is due to its failure to recruit IRAK-4. J. Exp. Med. *197*, 263–268.

Chuang, T.H., and Ulevitch, R.J. (2004). Triad3A, an E3 ubiquitin-protein ligase regulating Toll-like receptors. Nat. Immunol. *5*, 495–502.

Diehl, G.E., Yue, H.H., Hsieh, K., Kuang, A.A., Ho, M., Morici, L.A., Lenz, L.L., Cado, D., Riley, L.W., and Winoto, A. (2004). TRAIL-R as a negative regulator of innate immune cell responses. Immunity *21*, 877–889.

Divanovic, S., Trompette, A., Atabani, S.F., Madan, R., Golenbock, D.T., Visintin, A., Finberg, R.W., Tarakhovsky, A., Vogel, S.N., Belkaid, Y., et al. (2005). Negative regulation of Toll-like receptor 4 signaling by the Toll-like receptor homolog RP105. Nat. Immunol. *6*, 571–578.

Eriksson, U., Ricci, R., Hunziker, L., Kurrer, M.O., Oudit, G.Y., Watts, T.H., Sonderegger, I., Bachmaier, K., Kopf, M., and Penninger, J.M.

(2003). Dendritic cell-induced autoimmune heart failure requires cooperation between adaptive and innate immunity. Nat. Med. *9*, 1484–1490.

Fiorini, E., Schmitz, I., Marissen, W.E., Osborn, S.L., Touma, M., Sasada, T., Reche, P.A., Tibaldi, E.V., Hussey, R.E., Kruisbeek, A.M., et al. (2002). Peptide-induced negative selection of thymocytes activates transcription of an NF-kappa B inhibitor. Mol. Cell *9*, 637–648.

Fukao, T., Tanabe, M., Terauchi, Y., Ota, T., Matsuda, S., Asano, T., Kadowaki, T., Takeuchi, T., and Koyasu, S. (2002). PI3K-mediated negative feedback regulation of IL-12 production in DCs. Nat. Immunol. *3*, 875–881.

Hirotani, T., Lee, P.Y., Kuwata, H., Yamamoto, M., Matsumoto, M., Kawase, I., Akira, S., and Takeda, K. (2005). The nuclear IkappaB protein IkappaBNS selectively inhibits lipopolysaccharide-induced IL-6 production in macrophages of the colonic lamina propria. J. Immunol. *174*, 3650–3657.

Honda, K., Yanai, H., Negishi, H., Asagiri, M., Sato, M., Mizutani, T., Shimada, N., Ohba, Y., Takaoka, A., Yoshida, N., and Taniguchi, T. (2005). IRF-7 is the master regulator of type-I interferon-dependent immune responses. Nature *434*, 772–777.

Iwasaki, A., and Medzhitov, R. (2004). Toll-like receptor control of the adaptive immune responses. Nat. Immunol. *5*, 987–995.

Kawai, T., Adachi, O., Ogawa, T., Takeda, K., and Akira, S. (1999). Unresponsiveness of MyD88-deficient mice to endotoxin. Immunity *11*, 115–122.

Kinjyo, I., Hanada, T., Inagaki-Ohara, K., Mori, H., Aki, D., Ohishi, M., Yoshida, H., Kubo, M., and Yoshimura, A. (2002). SOCS1/JAB is a negative regulator of LPS-induced macrophage activation. Immunity *17*, 583–591.

Kisielow, P., Bluthmann, H., Staerz, U.D., Steinmetz, M., and von Boehmer, H. (1988). Tolerance in T-cell-receptor transgenic mice involves deletion of nonmature CD4+8+ thymocytes. Nature *333*, 742–746.

Kitajima, S., Takuma, S., and Morimoto, M. (1999). Changes in colonic mucosal permeability in mouse colitis induced with dextran sulfate sodium. Exp. Anim. *48*, 137–143.

Kobayashi, K., Hernandez, L.D., Galan, J.E., Janeway, C.A., Jr., Medzhitov, R., and Flavell, R.A. (2002). IRAK-M is a negative regulator of Toll-like receptor signaling. Cell *110*, 191–202.

Kobayashi, M., Kweon, M.N., Kuwata, H., Schreiber, R.D., Kiyono, H., Takeda, K., and Akira, S. (2003). Toll-like receptor-dependent production of IL-12p40 causes chronic enterocolitis in myeloid cell-specific Stat3-deficient mice. J. Clin. Invest. *111*, 1297–1308.

Kuhn, R., Lohler, J., Rennick, D., Rajewsky, K., and Muller, W. (1993). Interleukin-10-deficient mice develop chronic enterocolitis. Cell *75*, 263–274.

Kuwata, H., Watanabe, Y., Miyoshi, H., Yamamoto, M., Kaisho, T., Takeda, K., and Akira, S. (2003). IL-10-inducible Bcl-3 negatively regulates LPS-induced TNF-alpha production in macrophages. Blood *102*, 4123–4129.

Lang, K.S., Recher, M., Junt, T., Navarini, A.A., Harris, N.L., Freigang, S., Odermatt, B., Conrad, C., Ittner, L.M., Bauer, S., et al. (2005). Toll-like receptor engagement converts T-cell autoreactivity into overt autoimmune disease. Nat. Med. *11*, 138–145.

Lawrence, T., Bebien, M., Liu, G.Y., Nizet, V., and Karin, M. (2005). IKKalpha limits macrophage NF-kappaB activation and contributes to the resolution of inflammation. Nature *434*, 1138–1143.

Leadbetter, E.A., Rifkin, I.R., Hohlbaum, A.M., Beaudette, B.C., Shlomchik, M.J., and Marshak-Rothstein, A. (2002). Chromatin-IgG complexes activate B cells by dual engagement of IgM and Toll-like receptors. Nature *416*, 603–607.

Li, Q., Lu, Q., Bottero, V., Estepa, G., Morrison, L., Mercurio, F., and Verma, I.M. (2005). Enhanced NF-(kappa)B activation and cellular function in macrophages lacking I(kappa)B kinase 1 (IKK1). Proc. Natl. Acad. Sci. USA *102*, 12425–12430.

Liew, F.Y., Xu, D., Brint, E.K., and O'Neill, L.A. (2005). Negative regulation of Toll-like receptor-mediated immune responses. Nat. Rev. Immunol. *5*, 446–458.

Michelsen, K.S., Wong, M.H., Shah, P.K., Zhang, W., Yano, J., Doherty, T.M., Akira, S., Rajavashisth, T.B., and Arditi, M. (2004). Lack of Toll-like receptor 4 or myeloid differentiation factor 88 reduces atherosclerosis and alters plaque phenotype in mice deficient in apolipoprotein E. Proc. Natl. Acad. Sci. USA *101*, 10679–10684.

Moore, K.W., de Waal Malefyt, R., Coffman, R.L., and O'Garra, A. (2001). Interleukin-10 and the interleukin-10 receptor. Annu. Rev. Immunol. *19*, 683–765.

Motoyama, M., Yamazaki, S., Eto-Kimura, A., Takeshige, K., and Muta, T. (2005). Positive and negative regulation of nuclear factor-kappaB-mediated transcription by IkappaB-zeta, an inducible nuclear protein. J. Biol. Chem. *280*, 7444–7451.

Nakagawa, R., Naka, T., Tsutsui, H., Fujimoto, M., Kimura, A., Abe, T., Seki, E., Sato, S., Takeuchi, O., Takeda, K., et al. (2002). SOCS-1 participates in negative regulation of LPS responses. Immunity *17*, 677–687.

Natoli, G., Saccani, S., Bosisio, D., and Marazzi, I. (2005). Interactions of NF-kappaB with chromatin: the art of being at the right place at the right time. Nat. Immunol. *6*, 439–445.

Pasare, C., and Medzhitov, R. (2004). Toll-dependent control mechanisms of CD4 T cell activation. Immunity *21*, 733–741.

Saccani, S., Marazzi, I., Beg, A.A., and Natoli, G. (2004). Degradation of promoter-bound p65/RelA is essential for the prompt termination of the nuclear factor kappaB response. J. Exp. Med. *200*, 107–113.

Sakaguchi, S., Negishi, H., Asagiri, M., Nakajima, C., Mizutani, T., Takaoka, A., Honda, K., and Taniguchi, T. (2003). Essential role of IRF-3 in lipopolysaccharide-induced interferon-beta gene expression and endotoxin shock. Biochem. Biophys. Res. Commun. *306*, 860–866.

Strober, W., Fuss, I.J., and Blumberg, R.S. (2002). The immunology of mucosal models of inflammation. Annu. Rev. Immunol. *20*, 495–549.

Takaoka, A., Yanai, H., Kondo, S., Duncan, G., Negishi, H., Mizutani, T., Kano, S., Honda, K., Ohba, Y., Mak, T.W., and Taniguchi, T. (2005). Integral role of IRF-5 in the gene induction programme activated by Toll-like receptors. Nature *434*, 243–249.

Takeda, K., Clausen, B.E., Kaisho, T., Tsujimura, T., Terada, N., Forster, I., and Akira, S. (1999). Enhanced Th1 activity and development of chronic enterocolitis in mice devoid of Stat3 in macrophages and neutrophils. Immunity *10*, 39–49.

Wald, D., Qin, J., Zhao, Z., Qian, Y., Naramura, M., Tian, L., Towne, J., Sims, J.E., Stark, G.R., and Li, X. (2003). SIGIRR, a negative regulator of Toll-like receptor-interleukin 1 receptor signaling. Nat. Immunol. *4*, 920–927.

Wessells, J., Baer, M., Young, H.A., Claudio, E., Brown, K., Siebenlist, U., and Johnson, P.F. (2004). BCL-3 and NF-kappaB p50 attenuate lipopolysaccharide-induced inflammatory responses in macrophages. J. Biol. Chem. *279*, 49995–50003.

Yamamoto, M., Sato, S., Hemmi, H., Hoshino, K., Kaisho, T., Sanjo, H., Takeuchi, O., Sugiyama, M., Okabe, M., Takeda, K., and Akira, S. (2003). Role of adaptor TRIF in the MyD88-independent toll-like receptor signaling pathway. Science *301*, 640–643.

Yamamoto, M., Yamazaki, S., Uematsu, S., Sato, S., Hemmi, H., Hoshino, K., Kaisho, T., Kuwata, H., Takeuchi, O., Takeshige, K., et al. (2004). Regulation of Toll/IL-1-receptor-mediated gene expression by the inducible nuclear protein IkappaBzeta. Nature *430*, 218–222.

DNA Augments Antigenicity of Mycobacterial DNA-Binding Protein 1 and Confers Protection against *Mycobacterium tuberculosis* Infection in Mice[1]

Sohkichi Matsumoto,[2]* Makoto Matsumoto,† Kiyoko Umemori,‡§ Yuriko Ozeki,*¶ Makoto Furugen,‖ Tomishige Tatsuo,† Yukio Hirayama,* Saburo Yamamoto,‡ Takeshi Yamada,‖ and Kazuo Kobayashi*

Mycobacterium **consists up to 7% of mycobacterial DNA-binding protein 1 (MDP1) in total cellular proteins. Host immune responses to MDP1 were studied in mice to explore the antigenic properties of this protein. Anti-MDP1 IgG was produced after infection with either bacillus Calmette-Guérin or *Mycobacterium tuberculosis* in C3H/HeJ mice. However, the level of Ab was remarkably low when purified MDP1 was injected. MDP1 is considered to be associated with DNA in nucleoid, which contains immunostimulatory CpG motif. Therefore, we examined coadministration of MDP1 and DNA derived from *M. tuberculosis*. Consequently, this procedure significantly enhanced the production of MDP1-specific IgG. Five nanograms of DNA was enough to enhance MDP1-specific IgG production in the administration of 5 μg of MDP1 into mice. Strong immune stimulation by such a small amount of DNA is noteworthy, because >1,000- to 100,000-fold doses of CpG DNAs are used for immune activation. A synthetic peptide-based study showed that B cell epitopes were different between mice administered MDP1 alone and those given a mixture of MDP1 and DNA, suggesting that DNA alters the three-dimensional structure of MDP1. Coadministration of DNA also enhanced MDP1-specific IFN-γ production and reduced the bacterial burden of a following challenge of *M. tuberculosis*, showing that MDP1 is a novel vaccine target. Finally, we found that MDP1 remarkably enhanced TLR9-dependent immune stimulation by unmethylated CpG oligo DNA in vitro. To our knowledge, MDP1 is the first protein discovered that remarkably augments the CpG-mediated immune response and is a potential adjuvant for CpG DNA-based immune therapies.** ***The Journal of Immunology*****, 2005, 175: 441–449.**

Tuberculosis is a disease caused by infection with *Mycobacterium tuberculosis* and remains a serious threat to health in the world. Annually, 8 million people contract tuberculosis, and nearly 2 million people die from the disease. Worldwide, 32% of the population is persistently infected with *M. tuberculosis*, and some of these bacteria are thought to be in a nonreplicating dormant state (1). The majority of the disease arises from reactivation of persisting, previously implanted bacteria (2–5).

Bacillus Calmette-Guérin (BCG)[3] is an attenuated live vaccine against tuberculosis and has been given to >2 billion individuals to date. BCG is safe, inexpensive, and effective against both meningitis and miliary tuberculosis in infants, but frequently fails to protect from the most prevalent form of the disease, adult pulmonary tuberculosis (6–9). In addition, there is the possibility of causing opportunistic disease in immunocompromised hosts, such as AIDS patients, because BCG is a live vaccine and can survive in the hosts. Accordingly, there is an urgent need to develop a more effective and safer vaccine than BCG. Extensive studies to date have evaluated possible vaccine candidate proteins, such as a 6-kDa early secretory antigenic target (10); Ag 85 complexes A, B, and C (11); MTB39 and MTB48 (12); and heat shock protein 60 (13).

Mycobacterial DNA-binding protein 1 (MDP1) is produced by the genus *Mycobacterium* and is a major cellular protein, consisting of up to 7% of the total cellular protein (14). MDP1 has nucleic acid-binding activity mediated through interaction with guanine and cytosine residues in DNA (14, 15). Thus, MDP1 is presumed to be a component of the mycobacterial nucleoid and has been shown to localize to the 50S ribosomal subunit and on the bacterial surface (14, 16). The cellular content of MDP1 is increased in the stationary growth phase of mycobacteria relative to the exponential growth phase (14). Dick et al. (17) found that histone-like protein (HLP), the homologue of MDP1, was substantially upregulated in the dormant state of *Mycobacterium smegmatis*. Our previous study showed that MDP1 inhibited macromolecular biosyntheses in vitro and substantially suppressed bacterial growth (18). Taken together, it is conceivable that MDP1 has fundamental

Department of *Host Defense, Osaka City University Graduate School of Medicine, Osaka, Japan; †Microbiological Research Institute, Otsuka Pharmaceutical, Tokushima, Japan; Departments of ‡Bacterial Pathogenesis and Infection Control and §Safety Research on Blood and Biological Products, National Institute of Infectious Diseases, Tokyo, Japan; ¶Osaka International College, Osaka, Japan; and ‖Nagasaki University Graduate School of Biomedical Sciences, Nagasaki, Japan

Received for publication January 5, 2005. Accepted for publication April 16, 2005.

The costs of publication of this article were defrayed in part by the payment of page charges. This article must therefore be hereby marked *advertisement* in accordance with 18 U.S.C. Section 1734 solely to indicate this fact.

[1] This work was supported by grants from Japan Health Sciences Foundation; Ministry of Health, Labour and Welfare (Research on Emerging and Re-Emerging Infectious Diseases, Health Sciences Research Grants); Inamori Foundation; Ministry of Education, Culture, Sports, Science, and Technology; Osaka City University Urban Research; Osaka Tuberculosis Foundation; and the United States-Japan Cooperative Medical Science Program against Tuberculosis and Leprosy.

[2] Address correspondence and reprint requests to Dr. Sohkichi Matsumoto, Department of Host Defense, Osaka City University Graduate School of Medicine, 1-4-3 Asahi-machi, Abeno-ku, Osaka 545-8585, Japan. E-mail address: sohkichi@med.osaka-cu.ac.jp

[3] Abbreviations used in this paper: BCG, bacillus Calmette-Guérin; Ag85B, Ag 85 complex B; HLP, histone-like protein; HLP*Mt*, histone-like protein of *Mycobacterium tuberculosis*; HrpA, heat stress-induced ribosome-binding protein A; KO, knockout; LBP-21, laminin-binding protein of 21 kDa; Me-oligo B, synthetic oligo DNA containing methylated CpG sequence; MDP1, mycobacterial DNA-binding protein 1; ODN, synthetic oligodeoxynucleotide; PPD, purified protein derivative; RIB, RIBI adjuvant system; rMDP1, recombinant histidine-tagged MDP1.

0022-1767/05/$02.00

roles in the suppression of growth from both stationary and dormant phases of mycobacteria.

Of interest, MDP1 localizes on the bacterial surface as well as intracellularly (14, 16, 19, 20). During host-bacterium interaction, MDP1 may play a role as an adhesin. Shimoji et al. (20) found that a 21-kDa protein could bind to laminin-2, which is thought to be an *Mycobacterium leprae* receptor involved in attachment to Schwann cells (21). They designated this protein as laminin-binding protein of 21 kDa (LBP-21) and showed it to be a homologue of MDP1 in *M. leprae*, although it was deficient for DNA-binding activity (20). Thus, LBP-21 may have a role in the invasion of *M. leprae* into peripheral nerves, presumably cooperating with another adhesion molecule, phenolic glycolipid-1 (22). In addition to laminin, we recently found that MDP1 binds to glycosaminoglycans (16), which are a major component of the extracellular matrix. Glycosaminoglycans are important in the attachment of mycobacteria, especially in the interaction with nonphagocytic cells such as fibroblasts and epithelial cells (23), which are possible reservoirs of persisting *M. tuberculosis* in healthy humans (24).

Prasad et al. (25) used T cell blot assay to identify an immunodominant protein in healthy contacts with tuberculosis patients. They designated that protein as histone-like protein of *M. tuberculosis* (HLP*Mt*), which is the same molecule as MDP1. Both humoral and lymphoproliferative responses against recombinant HLP*Mt*/MDP1 were greater in healthy tuberculin reactors than in nonreactors or tuberculosis patients (25). This suggests that HLP*Mt*/MDP1 is an immunodominant Ag that may have an important role in host defense.

In this study we report a series of studies that analyze the antigenicity of MDP1 in a mouse model. We show that both humoral and cellular immune responses to MDP1 are stimulated by the presence of bacterial DNA that contains immunostimulatory CpG motifs (26, 27) that initiate immune responses through TLR9 (28). Simultaneous immunization with MDP1 and DNA, but not MDP1 alone, promotes protection against an *M. tuberculosis* challenge. An in vitro study demonstrated that a complex of MDP1 and CpG DNA markedly stimulates the production of proinflammatory cytokines in a TLR9-dependent manner. Proteins produced by pathogenic organisms are major targets of host immune responses that lead to protective immunity. Our data demonstrate that immunostimulatory cellular components that interact with these proteins have significant effects on protein recognition by the host and the subsequent development of protective immunity.

Materials and Methods

Mice

Female A/J, BALB/c, C3H/HeJ, and C57BL/6 mice were purchased from Japan SLC at 5–7 wk of age. TLR9 knockout (KO) mice (B6 129F2 background) were supplied by Dr. S. Akira (Osaka University, Osaka, Japan) (28). All mice were kept under specific pathogen-free conditions.

Bacterial strains and culture

BCG (strain Tokyo) was grown at 37°C in Middlebrook 7H9 media (Difco) supplemented with 10% albumin, dextrose, and catalase enrichment (Difco) and 0.05% Tween 80. When the OD at 630 nm was ~0.5, bacteria were collected by centrifugation and suspended in sterilized water to adjust for an OD of 1.0. Mice were infected i.p. with 5–10 × 10^6 CFU of BCG in 0.2 ml of normal saline. Two weeks later, mice were boosted with the same dose of BCG i.p. The bacterial dose was determined by counting CFUs 3 wk after plating serial 10-fold dilutions of suspension onto Middlebrook 7H11 agar containing oleic acid, dextrose, albumin, and catalase enrichment (Difco; 7H11-OADC agar).

Antigens

Recombinant histidine-tagged MDP1 (rMDP1) was purified from *Escherichia coli* transfected with pET21b$^+$-*mdp1* by methods described previously (16). Native MDP1 was purified from BCG (Tokyo strain) using the method described previously (14). Ag 85 complex B (Ag85B) purified from *M. tuberculosis* H37Rv was a gift from Dr. S. Nagai (29). Heat stress-induced ribosome-binding protein A (HrpA), purified as a recombinant protein (30), was supplied by Drs. N. Ohara and T. Tabira (Nagasaki University, Nagasaki, Japan). Bovine histone H1, histone H2A, and histone H3 were purchased from Roche. Bacterial DNA was purified from *M. tuberculosis* H37Rv by phenol-chloroform extraction (31). Briefly, 5 g of *M. tuberculosis* H37Rv (wet weight) was suspended in 5 ml of 10 mM Tris-HCl and 1 mM EDTA (pH 7.5; TE buffer), mixed with the same volume of chloroform/methanol (2/1), and incubated for 5 min to remove lipids. The suspension was centrifuged at 2,500 × *g* for 20 min, and both organic and aqueous layers were decanted to leave a packed bacterial band. Delipidated bacteria were incubated at 55°C for 20 min to remove traces of organic solvents and were resuspended in 5 ml of TE buffer and 0.5 ml of 1 M Tris-HCl (pH 9.6). Lysozyme (Sigma-Aldrich) was added to a final concentration of 100 μg/ml and incubated for 2 h. Then 0.1 vol of 10% SDS and 0.01 vol of proteinase K (Sigma-Aldrich) were added and additionally incubated overnight. To remove contaminating proteins, the same volume of phenol was added, gently mixed for 20 min, and centrifuged at 12,000 × *g* for 20 min. The aqueous layer was transferred to the fresh tube, and the protein-removing step was repeated again. Then the same volume of chloroform/isoamyl alcohol (24/1) was added and gently mixed for 10 min. The tube was centrifuged at 12,000 × *g* for 10 min, then the supernatant was transferred to new tube. DNA was precipitated by gently mixing after adding 0.1 vol of 3 M sodium acetate (pH 5.2) and 2.5 vol of ethanol. The tube was then centrifuged at 12,000 × *g* for 10 min, and the DNA pellet was rinsed with 70% ethanol. The pellet was resolved in pure water, and the concentration was determined by the absorbance at 260 nm. The endotoxin level of Ags was <50 pg/100 μM, as determined by a *Limulus* test.

Immunization of mice with protein Ags and BCG

Protein Ags were emulsified using the RIBI adjuvant system (RIB; Corixia), which consists of synthetic trehalose dicorynomycolate and monophosphoryl lipid A, or by IFA (Difco). In some cases, Ags were mixed with various amounts of DNA for 10 min at 37°C and then emulsified. Five micrograms of protein with or without DNA was injected i.p. Three weeks later, mice were boosted using the same method as the primary immunization. The same protocol was used for BCG immunization. Five to 10 × 10^6 CFU of BCG was i.p. injected per mouse. Three weeks after the boost, peripheral blood was obtained from the retro-orbital plexus of anesthetized mice, and sera were isolated and stored at −80°C until the assays.

Western blot

One microgram of purified MDP1 was fractionated by SDS-PAGE, transferred to a polyvinylidene difluoride membrane, and reacted with antisera diluted 1/200.

ELISA

Ninety-six-well ELISA plates (Sumitomo) were coated with individual protein Ags, such as MDP1, HrpA, Ag85B, histone H1, histone H2A, and histone H3, by overnight incubation in carbonate buffer (pH 9.6) at 4°C. Wells were then blocked by PBS containing 3% BSA for 2 h at room temperature. Equal volumes of sera from at least five mice were mixed in each experimental group. Sera were serially diluted in PBS containing 1% BSA, added to wells, and incubated overnight at 4°C. The wells were washed four times with PBS containing 0.05% Tween 20, and HRP-conjugated goat anti-mouse IgG (DakoCytomation), IgG1, IgG2a, IgG2b, IgG3 (Santa Cruz Biotechnology), or IgG2c (Bethyl) diluted in PBS containing 1% BSA was added and incubated for 2 h at room temperature. After washing as before, 100 μl of 80 mM citrate-phosphate buffer (pH 5.0) containing 0.4 μg/ml *o*-phenylendiamine dihydrochloride (Wako Pure Chemicals) was added to the wells, and absorbance at 492 nm was measured by an MTP-300 microplate reader (Corona Electronic).

To determine B cell epitopes, overlapping peptides covering the entire sequence of MDP1 were synthesized previously as 20-mer molecules with 10-aa overlaps with the neighboring peptides, with exception of the C-terminal (15). Each peptide was dissolved in PBS at a concentration of 10 μg/ml and immobilized onto type A ELISA plates (Sumitomo) after activation of the wells by 2% glutaraldehyde. Sera diluted 1/200 by PBS containing 0.05% Tween 20 was added and incubated at 4°C overnight. The ELISA procedure described above was performed, and B cell epitopes were defined by color development with *o*-phenylendiamine dihydrochloride.

Lymph node cell culture and stimulation

Mice were killed 3 wk after the booster injection of Ags, and mesenteric lymph node cells were prepared. Cells were cultured in RPMI 1640 medium (Sigma-Aldrich) supplemented with 10% FBS (Sigma-Aldrich), 25 mM HEPES, 2 mM L-glutamine, 5.5×10^{-5} M 2-ME, 100 U/ml penicillin, and 100 μg/ml streptomycin (complete RPMI medium) in the presence or the absence of 10 μg/ml, MDP1, Ag85B, or purified protein derivative (PPD; Kyowa) in a humidified incubator at 37°C under 5% CO_2. IFN-γ in the culture supernatant was measured with ELISA kits (Genzyme Techne).

Prior immunization and challenge with M. tuberculosis

C3H/HeJ or BALB/c mice were s.c. immunized with 5 μg of RIB-emulsified MDP1 with or without 5 ng of *M. tuberculosis* DNA, DNA alone (5 ng), or 5 μg of Ag85B. BCG Tokyo at a dose of 10^6 CFUs was inoculated using the same procedure without emulsification. After 3 wk, mice were boosted i.p. by the same Ags and were challenged 3 wk later i.v. with 1×10^6 CFU of *M. tuberculosis* Kurono strain (ATCC 35812; American Type Culture Collection). On days 14 and 28, lungs were removed and homogenized using an LS-50 homogenizer (Yamato). The lung homogenates were serially diluted and inoculated onto 7H11-OADC agars. Bacterial numbers were calculated and expressed as CFU.

Spleen cell culture and stimulation

Synthetic oligodeoxynucleotides (ODNs) of sequence GGGGGGAACGT TGGGGGGGGGGGGGGGGG were purchased from Nisshinbo and designated oligo B. As a control, cytosine-methylated oligo B was synthesized (Me-oligo B). The endotoxin level was <50 pg/100 μM, as determined by a *Limulus* test. Spleens obtained from C57BL/6 and TLR9 KO mice were cut into small pieces and homogenized. These cell suspensions were depleted of erythrocytes using a Ficoll gradient (Lympholyte-M; Cedarlane Laboratories) and centrifuged for 20 min at 1000 × *g* at room temperature. Spleen cells (1×10^6 cells/well) were cultured in the presence or the absence of MDP1 and ODNs at final concentrations of 0.5 and 1 μM, respectively. After 10-min incubation at 37°C, the MDP1-ODN mixture was added to the cell cultures and incubated for 24 h. As a control, cells were also stimulated with LPS derived from *E. coli* 0111 134 (Difco) at concentration of 100 ng/ml. The amounts of TNF-α and IL-6 in the culture supernatants were measured with ELISA kits (Genzyme Techne).

Statistical analyses

Statistical analysis was conducted with a Power Macintosh G4 using StatView 5.0 (SAS Institute). ANOVA was used to determine the significance of differences in means between multiple experimental groups. The significance level of the test was <5%.

Results

Anti-MDP1 IgG production in mice

To explore the antigenicity of MDP1, we first analyzed the humoral immune response to MDP1 in mice. BCG was inoculated into three strains of mice, including A/J, BALB/c, and C3H/He. Western blot analysis showed that MDP1 elicited a humoral immune response in all strains (Fig. 1*A*). Sera from nonimmunized mice did not react with MDP1 (data not shown). Additionally, anti-MDP1 IgG was produced in C3H/He and BALB/c mice challenged with *M. tuberculosis* H37Rv (data not shown).

We next assessed the antigenicity of purified MDP1. Five micrograms of MDP1 was emulsified in RIB and injected into C3H/He mice. In contrast to inoculation of BCG, we could not detect a significant level of anti-MDP1 IgG (Fig. 1*A*). MDP1 presumably binds to DNA, which includes immunostimulatory CpG motifs (27). Therefore, we tested the simultaneous administration of MDP1 and DNA. Five micrograms of MDP1 was incubated with 0.5 μg of DNA derived from *M. tuberculosis* H37Rv, and the mixture was injected into C3H/He mice. Western blot analysis showed that a combination of MDP1 and DNA elicited MDP1-specific IgG production, whereas MDP1 or DNA alone did not (Fig. 1*A*).

We next determined the optimal dose of DNA that could enhance anti-MDP1 IgG production. Using RIB, 5 μg of MDP1 was administered to C3H/He mice with or without 10-fold serial dilutions of DNAs ranging from 5 μg to 5 ng. Three weeks after the booster injection, the level of anti-MDP1 IgG was measured by ELISA (Fig. 1*B*). The production of IgG was dependent on the amount of DNA; interestingly, 5 ng of DNA most efficiently stimulated IgG production against MDP1. We observed enhanced anti-MDP1 IgG production by coadministration of DNA and MDP1 in the presence of IFA (Fig. 1*C*), and the result was similar to that

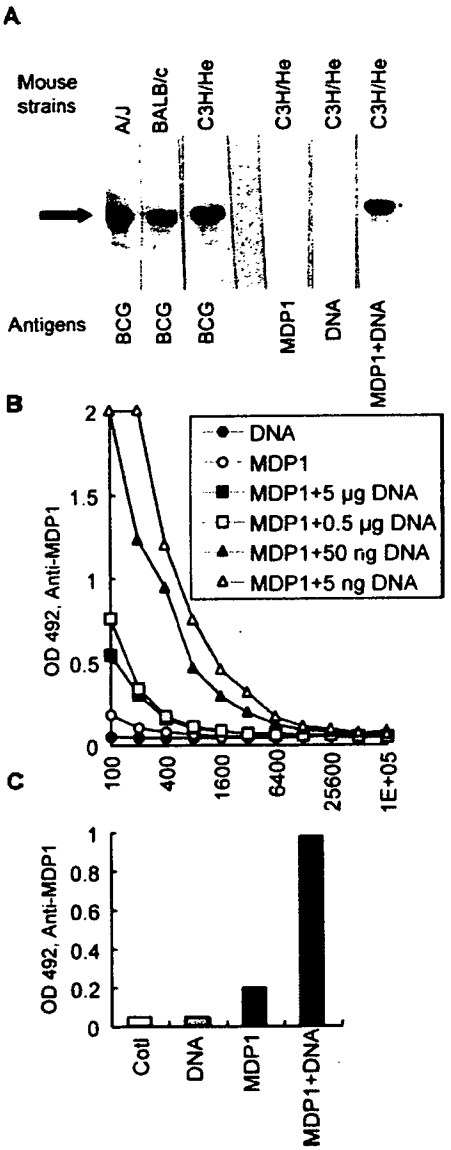

FIGURE 1. Humoral immune responses to MDP1 in mice. *A*, Western blot analysis. Purified MDP1 was blotted onto the membrane and incubated with 200/1 diluted antisera. Mouse strains are indicated along the *top* of the panel. The injected Ags, such as BCG, MDP1 alone (MDP1), *M. tuberculosis* DNA alone (DNA), and MDP1 plus DNA (MDP1+DNA) are shown along the *bottom*. *B*, DNA dose effects on anti-MDP1 IgG production. C3H/He mice were immunized with MDP1 (5 μg/mouse) with or without various amounts of DNA (5 μg to 5 ng) emulsified in RIB adjuvant, and levels of anti-MDP1 IgG were determined by ELISA. The horizontal axis shows dilution factors of antisera. *C*, Immunization with MDP1 plus DNA emulsified in IFA augmented anti-MDP1 IgG production. C3H/He mice were immunized with Ags emulsified in IFA. Immunized Ags are described *below* the horizontal axis. Cotl, IFA alone. The sera from at least five mice of each experimental group were mixed and diluted to 1/400, and the levels of anti-MDP1 IgG were determined by ELISA.

observed using RIB adjuvant, suggesting that the immunostimulatory effect of DNA on anti-MDP1 IgG production is not restricted to RIB adjuvant. The results prompted us to explore whether DNA-dependent IgG production varies between mouse strains. The same immunization procedure using RIB as an adjuvant was performed in other mouse strains, including A/J, BALB/c, and C57BL/6. The results revealed that simultaneous inoculation of MDP1 and DNA augmented the production of IgG against MDP1 in all tested strains (Fig. 2).

To determine whether DNA-mediated enhancement of anti-MDP1 IgG production is restricted to the particular IgG isotype, we analyzed the distribution of subclasses of IgG by ELISA. As shown in Fig. 3, each mouse strain possessed a specific pattern of MDP1-specific IgG isotypes, but DNA enhanced only IgG subclasses produced in mice immunized with MDP1 alone. Thus, a small dose of DNA augments the humoral response to MDP1 without altering the pattern of IgG isotypes.

MDP1-specific, DNA-dependent stimulation of IgG production

Our data showed that a small amount of DNA (5 ng) magnified anti-MDP1 IgG production (Fig. 1*B*). In contrast, 1,000- to 100,000-fold higher amounts (5–500 μg) of bacterial DNA and CpG ODNs have been applied as adjuvants in immunization with foreign Ags (32–34) or immunotherapeutic treatments (34–38). Therefore, we next examined whether 5 ng of DNA stimulated Ab production against other immunogenic mycobacterial proteins such as HrpA (39) and Ag85B (11). These Ags did not bind to DNA, as determined by gel retardation assay (data not shown). Five micrograms of each Ag was injected into BALB/c, C3H/He, and C57BL/6 mice, with or without 5 ng of DNA. We could not detect enhanced Ab production by coadministration of DNA in any of the three mouse strains (Fig. 4, *A* and *B*).

Next we examined whether DNA combined with DNA-binding proteins other than MDP1 stimulates IgG production. Bovine histone H1, histone H2A, and histone H3 were injected into three strains of mouse (BALB/c, C3H/He, and C57BL/6) with or without 5 ng of DNA. We could not detect the production of IgG against both histones H2A and H3 in any of mouse strains tested (data not shown). In contrast, anti-histone H1 Ab was detectable in all mouse strains, but DNA alone did not stimulate anti-histone H1 IgG production (Fig. 4*C*). Although we have not tested all DNA-binding proteins, these results imply that enhanced Ab production by a very small amount of bacterial DNA is a unique feature of MDP1.

DNA alters B cell epitopes of MDP1

To examine humoral immune responses against MDP1 more precisely, we defined the region(s) recognized by anti-MDP1 IgG. B cell epitope mapping was conducted by ELISA using synthetic 20-mer peptides covering the entire MDP1 sequence. Antisera were obtained from four strains of mice, including A/J, BALB/c, C3H/He, and C57BL/6, immunized with MDP1 alone or with 5 ng of DNA and were reacted with each peptide. In A/J mice, IgG from animals immunized with MDP1 alone did not react with peptides, although it was bound to MDP1, suggesting that IgG in these mice recognized the conformational structure of MDP1 (Fig. 5*A*). In contrast, two peptides corresponding to aa 61–80 and 71–90 of MDP1 were recognized by anti-MDP1 IgG in mice immunized with MDP1 plus DNA (Fig. 5*A*). In BALB/c mice, anti-MDP1 IgG induced by injection of both MDP1 alone and MDP1 plus DNA reacted with the peptide corresponding to 51–70 of MDP1 (Fig. 5*B*). In C3H/He mice, the level of anti-MDP1 IgG was insignificant when MDP1 alone was used (Fig. 5*C*). In contrast, anti-MDP1 IgG was produced in animals immunized with MDP1 plus DNA and reacted with peptides corresponding to 141–160 and 151–170 (Fig. 5*C*). Thus, the epitope was likely to be the 151–160 region of MDP1. In C57BL/6 mice, Abs from mice immunized with MDP1 alone and MDP1 plus DNA reacted with the 61–80 and 1–20 regions, respectively (Fig. 5*D*).

Although the anti-MDP1 Ab titer was higher in BALB/c mice injected with MDP1 plus DNA than in mice immunized with

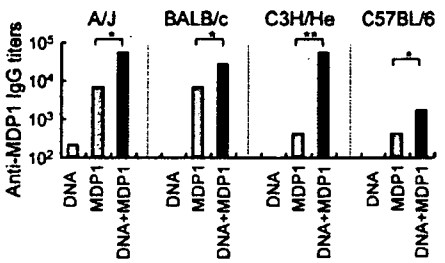

FIGURE 2. DNA stimulates the production of anti-MDP1-IgG in mice. Four strains of mice, including A/J, BALB/c, C3H/He, and C57BL/6, were immunized with DNA alone (□), MDP1 (5 μg/mouse) alone (▨), or MDP1 plus DNA (■). The titer of anti-MDP1-IgG was determined by ELISA. *, $p < 0.05$; **, $p < 0.01$ (by ANOVA).

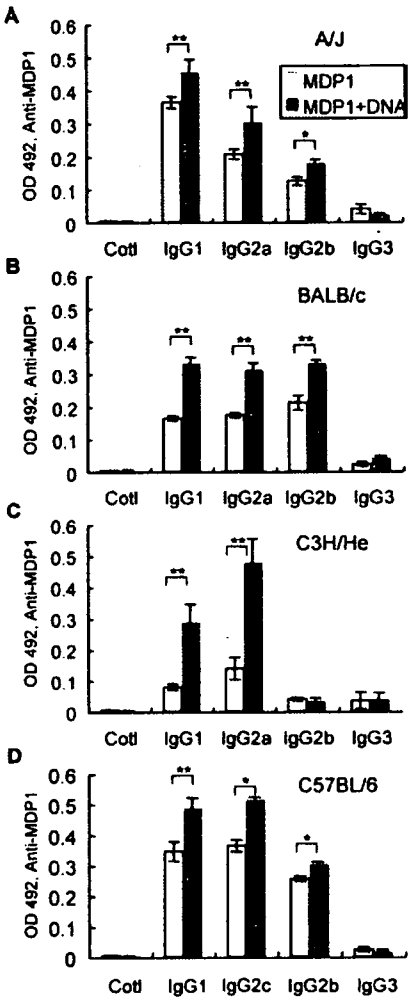

FIGURE 3. Isotypes of anti-MDP1 IgG. The levels of IgG subclasses were measured using isotype-specific Abs against IgG1, IgG2a, IgG2b, IgG2c, and IgG3. Cotl, Controls without secondary Ab. □, Immunization with MDP1 alone; ▨, coadministration of MDP1 and DNA. Antisera were diluted 1/100 (*A–C*) or 1/50 (*D*). *, $p < 0.05$; **, $p < 0.01$ (by ANOVA).

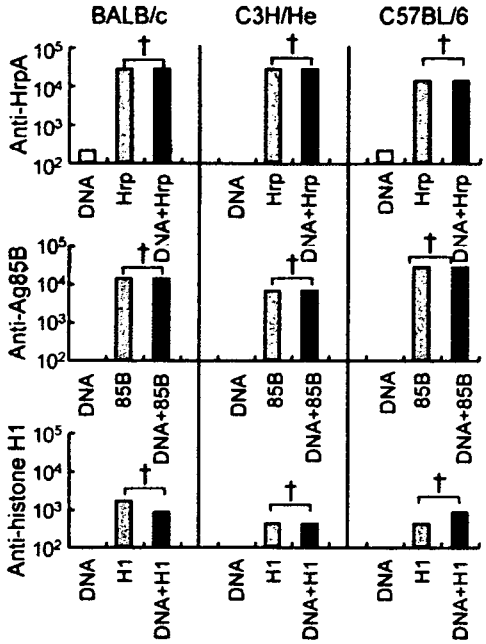

FIGURE 4. DNA fails to stimulate production of IgGs against mycobacterial Ags, HrpA and Ag85B, and a DNA-binding protein, histone H1. BALB/c, C3H/He, and C57BL/6 mice were immunized with 5 μg of HrpA (Hrp), Ag85B (85B), and histone H1 (H1) with (■) or without (▩) 5 ng of DNA. □, Immunization with DNA alone. The titer of Ag-specific IgG was measured by ELISA. †, $p > 0.1$ (by ANOVA).

MDP1 alone, the level of anti-MDP1 IgG against the defined epitope (aa 51–70) was reversed (Fig. 5*B*). This suggests that anti-MDP1 IgG recognizes mainly conformational epitopes in mice immunized with a mixture of MDP1 and DNA. To examine this possibility, inhibition assays were performed. The interaction between MDP1 and IgG from mice immunized with MDP1 alone (Fig. 6*A*), but not with MDP1-DNA (Fig. 6*B*), was inhibited by exogenously added peptide corresponding to aa 51–70 of MDP1 (Fig. 6, *A* and *B*). In contrast, the same molar amount of exogenously added MDP1 alone inhibited both reactions (Fig. 6, *A* and *B*). These data indicate that in BALB/c mice, administration of MDP1 alone produces IgG that recognizes only the 51–70 region. In contrast, administration of MDP1 plus DNA induces anti-MDP1 IgG targeting conformational epitopes on MDP1 in addition to the 51–70 region.

Similar inhibition experiments were conducted using sera from BALB/c mice injected with live BCG. The 51–70 peptide failed to abrogate the IgG-MDP1 interaction (Fig. 6*C*), although MDP1 itself did. This suggests that MDP1 is actually binding to DNA in vivo and is targeted by the host immune response.

MDP1 stimulates IFN-γ production

Protective immunity against *M. tuberculosis* infection is mediated primarily by Th1-type cell-mediated immunity (40, 41). IFN-γ triggers Th1-type cell-mediated immune responses and plays a critical role in host defense against *M. tuberculosis* infection in mice (42, 43). To investigate whether MDP1 participates in BCG-mediated protection against tuberculosis, we examined IFN-γ production induced by MDP1 stimulation. Lymph node cells from C3H/He mice immunized with BCG were cultured in the presence or the absence of MDP1, and the level of IFN-γ in culture supernatants was measured by ELISA. The results show that MDP1 stimulated IFN-γ production in a manner similar to Ag85B and PPD (Fig. 7*A*). We next examined isotypes of anti-MDP1 IgG in

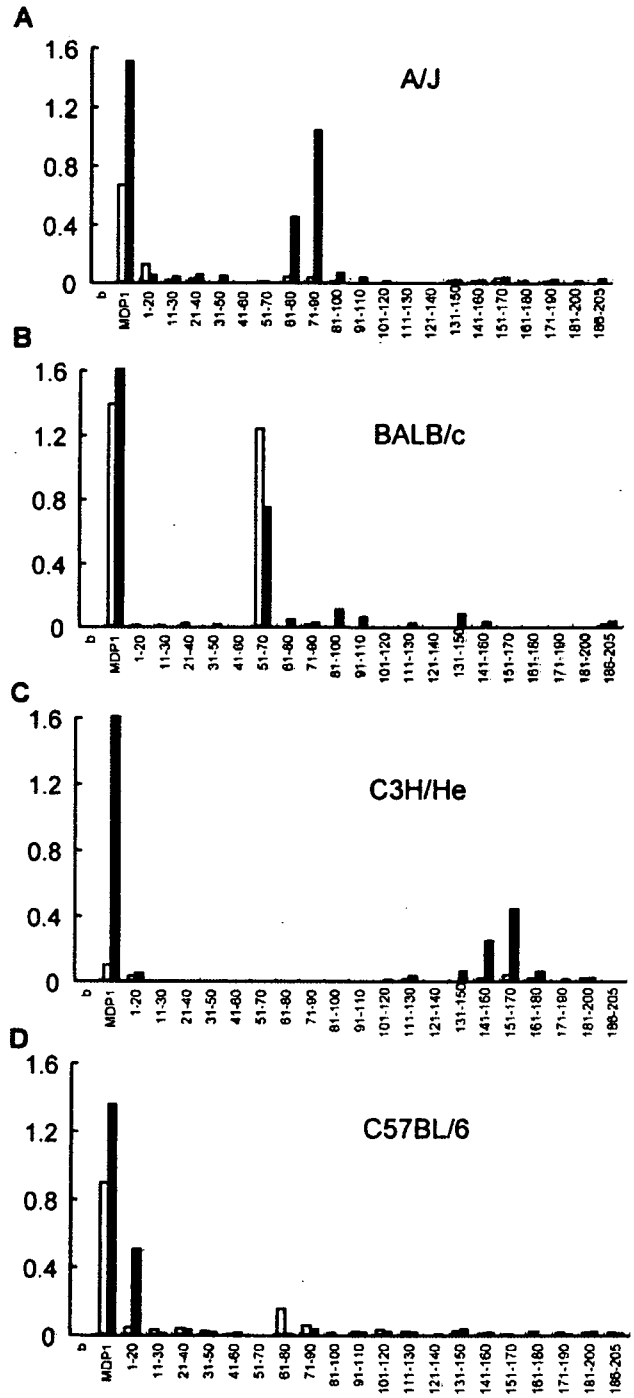

FIGURE 5. B cell epitope mapping of anti-MDP1 IgG. Epitopes of anti-MDP1 IgGs were determined by ELISA. MDP1 or 20-mer synthetic peptides covering the entire MDP1 sequence were coated on the ELISA plate as indicted at the *bottom* of each graph. b, Blank well without Ag coating. The same antisera as those described in Fig. 2 were diluted 1/200 and applied to the wells. *A–D*, Analysis of antisera derived from A/J, BALB/c, C3H/He, and C57BL/6 mice, respectively. □, Antisera from mice inoculated with MDP1 alone; ■, antisera from mice inoculated with MDP1 plus DNA. The ELISA units represent the average of duplicate samples.

BCG-immunized C3H/He mice. BCG inoculation stimulated the production of MDP1-specific IgG1 and IgG2a, but not IgG2b or IgG3 (Fig. 7*B*). Interestingly, the pattern of IgG isotypes was similar to that observed in the same mouse strain immunized with both

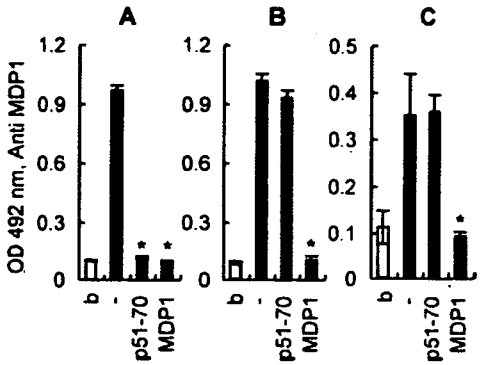

FIGURE 6. Production of anti-MDP1 IgG-targeting conformational epitopes in BALB/c mice immunized with MDP1 plus DNA or BCG, but not with MDP1 alone. Antisera from BALB/c mice immunized with MDP1 alone (*A*), MDP1 plus DNA (*B*), and BCG (*C*) were reacted with immobilized MDP1 on ELISA plates with or without exogenously added peptide corresponding to the 51–70 region of MDP1 (p51–70) or MDP1 (MDP1). b, Blank without Ag coating; −, positive controls without inhibitors. *, $p <$ 0.05 (by ANOVA, vs controls without inhibitors (−)).

MDP1 and DNA (Fig. 3*C*). IFN-γ induces IgG2a production (44), whereas both Th1-related and Th2 cytokines stimulate IgG1 production (45, 46). The predominant production of IgG2a implies that the immune response to MDP1 is polarized toward the Th1 type. It is likely that MDP1 is one of the Ags that induce protective immunity after BCG immunization in C3H/He mice.

Next we examined whether the administration of purified MDP1 induces IFN-γ production. C3H/He mice were immunized with MDP1 alone or with MDP1 plus DNA. As controls, RIB and DNA alone were administered to mice as well. Lymph node cells were cultured with or without 10 μg/ml MDP1, and the production of IFN-γ was assessed. The results showed that MDP1 stimulates IFN-γ production (Fig. 7*C*). However, immunization with MDP1 mixed with DNA produced much more IFN-γ than that with MDP1 alone, demonstrating that DNA augments cell-mediated immune responses to MDP1 (Fig. 7*C*).

Simultaneous administration of MDP1 and DNA confers protection against M. tuberculosis *infection in mice*

The ability to produce IFN-γ by MDP1 prompted us to explore whether MDP1 could induce protection in vivo against challenge with a virulent strain of *M. tuberculosis*. C3H/He mice were immunized with MDP1 alone or with MDP1 plus 5 ng of DNA. As controls, mice were given RIB alone, DNA alone, BCG, or Ag85B, which is a major vaccine candidate (11). After a 3-wk interval, mice were boosted with the same Ag; 3 wk later, mice were challenged with *M. tuberculosis* Kurono. After 14 and 28 days, mice were killed, and the numbers of bacteria in the lungs and spleens were determined. These data showed that immunization with Ag85B, DNA, and MDP1 failed to protect (Fig. 8, *A–C*). In contrast, BCG and coadministration of MDP1 and DNA significantly reduced the bacterial load in the lungs ($p < 0.005$ and $p =$ 0.0119 on day 14, and $p = 0.008$ and $p = 0.0316$ on day 28, respectively). A protective effect of immunization of MDP1 plus DNA, but not MDP1 alone, was also observed in the spleens ($p =$ 0.021; Fig. 8*C*). As shown in Fig. 8*D*, immunization with both MDP1 and DNA resulted in a modest, but significant, decrease in bacterial burden in BALB/c mice as well ($p < 0.005$). Although the effect was less than that of BCG, MDP1 confers substantial protection against *M. tuberculosis* challenge only when it is administered with DNA.

MDP1 augments TLR9-dependent immunostimulation by CpG DNA

Immunostimulatory effects of DNA are dependent on unmethylated CpG motifs (27) that signal via TLR9 (28). Our data revealed that a very small amount of DNA stimulates immune responses against MDP1, in contrast with previous reports (32–34). Therefore, we hypothesized that MDP1 might enhance the immunostimulatory activity of CpG DNA. To test this hypothesis, we evaluated the effect of MDP1 on CpG-ODN-mediated immune activation in vitro. Spleen cells from both C57BL/6 and TLR9 KO C57BL/6 mice were stimulated with oligo B containing CpG DNA sequence in the presence or the absence of rMDP1. Me-oligo·B, which has the same structure, except that its cytosine is methylated, and LPS, which signals via TLR4 (47, 48), were used as controls. After 24 h, levels of the proinflammatory cytokines TNF-α and IL-6 in the culture supernatants were determined by ELISA. Oligo B alone (1 μM) did not induce the production of TNF-α (Fig. 9). In contrast, the mixture of rMDP1 and oligo B dramatically stimulated TNF-α production (Fig. 9). This effect was undetectable in splenocytes from TLR9 KO mice or with the combination of Me-oligo B and rMDP1. Similar results were seen for

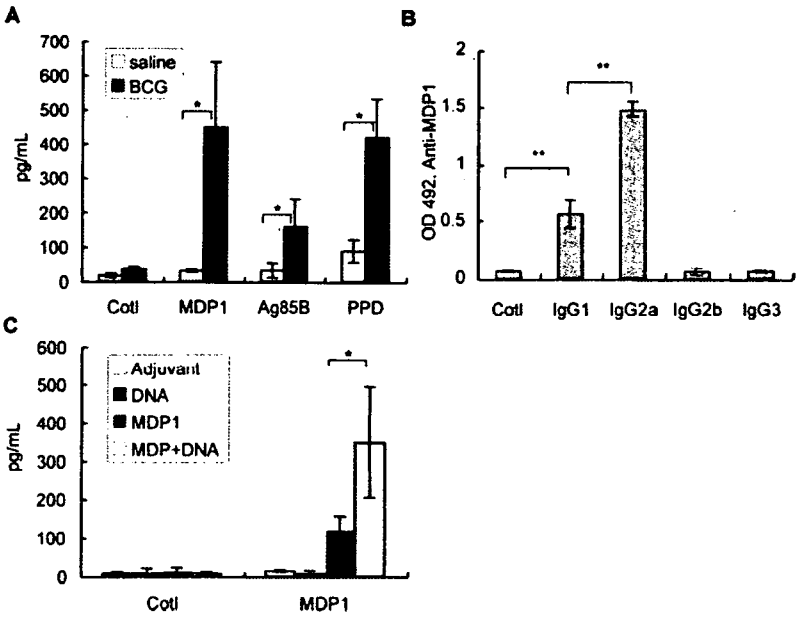

FIGURE 7. Development of Th1-type immune responses against MDP1 after challenge with BCG (*A* and *B*) or MDP1 (*C*). *A*, Amounts of IFN-γ in culture supernatants from lymph node cells were determined by ELISA. Lymph nodes were derived from C3H/He mice immunized with saline (□) or BCG (▨) and incubated for 5 days with 10 μg/ml MDP1, Ag85B, and PPD as indicated. Cotl, without Ag stimulation. The production of IFN-γ was measured by ELISA. *B*, MDP1-specific IgG isotypes (IgG1, IgG2a, IgG2b, and IgG3) in sera of C3H/He mice immunized with BCG detected by ELISA. Cotl, controls without secondary Ab. *C*, Lymph node cells derived from C3H/He mice immunized with adjuvant alone (□), DNA (■), MDP1 (▧), and MDP1 plus DNA (▨) were cultured in the presence (MDP1) or the absence (Cotl) of 10 μg/ml MDP1 for 5 days, and the amounts of IFN-γ in the culture supernatants were determined by ELISA. *, $p < 0.05$; **, $p < 0.01$ (by ANOVA).

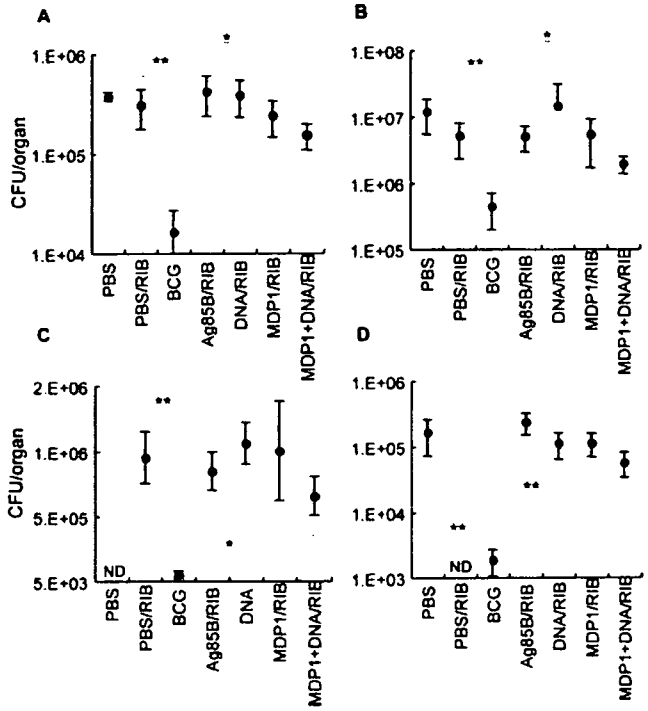

FIGURE 8. Coadministration of MDP1 and DNA confers protection against *M. tuberculosis* challenge. C3H/HeJ (*A–C*) and BALB/c (*D*) mice were immunized with Ags, as indicated below the horizontal axis, and challenged i.v. with 10^6 CFU of *M. tuberculosis* Kurono strain. Fourteen (*A*) and 28 (*B–D*) days after the challenge, bacterial numbers in lung (*A*, *B*, and *D*) and spleen (*C*) were determined by counting CFUs. *, $p < 0.05$; **, $p < 0.005$ (by ANOVA).

IL-6 production, although 0.5 μM rMDP1 itself induced a low level of IL-6 production (Fig. 9). Similar data were obtained when natural MDP1 was used under the same conditions (data not shown). These data clearly demonstrate that MDP1 activates TLR9-dependent immunostimulation by CpG ODN.

Discussion

In the present study we have evaluated the antigenicity of MDP1, a DNA-binding protein specific to mycobacteria. Anti-MDP1 IgG

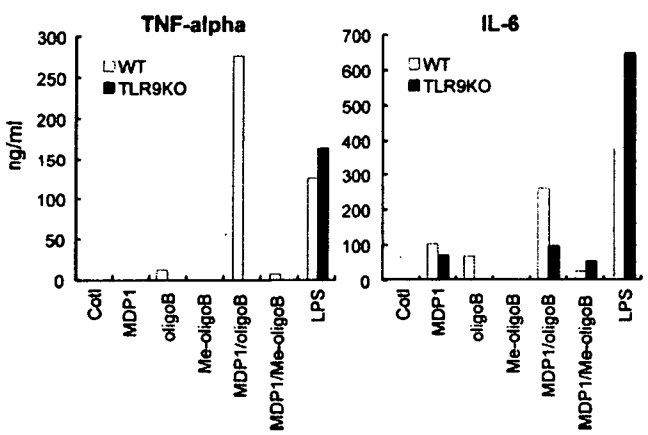

FIGURE 9. MDP1 enhances CpG-mediated production of proinflammatory cytokines in vitro. Splenocytes were stimulated with 0.5 μM MDP1 alone, a mixture of MDP1 and ODNs (1 μM), or *E. coli* LPS (100 ng/ml) for 24 h in vitro. Levels of TNF-α (*right*) and IL-6 (*left*) were determined by ELISA. The ELISA units represent the average of duplicate samples and are representative of two experiments performed.

was produced in C3H/He mice challenged with either BCG (Fig. 1*A*) or *M. tuberculosis* (data not shown). Marked cell proliferation occurred when splenocytes from *M. tuberculosis*-infected mice were stimulated with 10 μg/ml MDP1 in vitro. Uptake of [^{3}H]thymidine was higher compared with stimulation with the gold standard, PPD (our unpublished observations). Thus, in agreement with a human study (25), MDP1 is also highly immunogenic in mice.

However, administration of purified MDP1 failed to produce anti-MDP1-IgG in C3H/He mice (Fig. 1). This lack of antigenicity was reversed by adding mycobacterial DNA when immunizing with MDP1 (Fig. 1). Similarly, DNA enhanced the production of MDP1-specific IgG in other mouse strains (Fig. 2). B cell epitope mapping (Fig. 5*B*) and Ab reaction-inhibition assay (Fig. 6) implied association of MDP1 with genomic DNA in live BCG. These results suggest that the strong immunogenicity of MDP1 in mycobacterial infection is responsible for colocalization of DNA.

Studies to determine the optimal dose of DNA showed that 5 ng of DNA was enough to activate MDP1-specific IgG production (Fig. 1*B*). This dose is unusually low compared with other studies in which 5–500 μg of DNA or ODN/mouse was used for immune activation (32–34, 36–38). We confirmed that 5 ng of DNA did not enhance the production of IgG against other proteins, including DNA-binding proteins (Fig. 4). Thus, a very small amount of DNA-stimulated Ig production appears to be a specific feature of MDP1.

We determined B cell epitopes on MDP1 by using synthetic peptides. B cell epitopes differed among mouse strains. Surprisingly, the epitopes were different when DNA was coadministered with MDP1, even within the same mouse strain (Fig. 5). Thus, DNA not only stimulates MDP1-specific IgG production, but also modifies the recognition site of IgG. This suggests that the three-dimensional structure of MDP1 differs depending on whether DNA is present or absent, and this difference is recognized by the immune system of the host. This conformational change might be involved in the disparate antigenicities of this protein.

To investigate the role of MDP1 in host protection, we examined the activity of MDP1 in the induction of IFN-γ that is critical for host defense against *M. tuberculosis* infection in mice (42, 43). When stimulated in vitro with 10 μg/ml MDP1, lymph node cells derived from BCG-immunized C3H/He (Fig. 7*A*) and C57BL/6 (data not shown) mice produced a significant amount of IFN-γ. Analysis of IgG isotype in BCG-immunized mice revealed the production of MDP1-specific IgG2a, which was indicative of a Th1-type immune response (Fig. 7*B*) (44). Administration of purified MDP1 also expanded the population of IFN-γ-producing cells (Fig. 7*C*) and stimulated Th1-associated IgG2a production (Fig. 3). Again, simultaneous injection of MDP1 and DNA stimulated adaptive immunity and enhanced IFN-γ production (Fig. 7*C*). This was confirmed when mice were infected with *M. tuberculosis*, and MDP1 was found to decrease bacterial load only when coadministered with DNA (Fig. 8). Thus, MDP1 can be a novel vaccine target, although it is effective only when administered simultaneously with DNA. Because *M. tuberculosis* is transmitted by the aerogenic route, future studies are needed to explore the efficacy using the aerosol challenge model.

As discussed above, our data show that MDP1 has a unique feature as an Ag, in that its antigenicity is profoundly enhanced by even a small amount of DNA. This raises an important question as to how this immune stimulation is coordinated. At least six nucleotides are necessary for immune activation by ODN (49). Because DNA is highly sensitive to degradation by DNases, a large amount of DNA is required for immune activation (50). We found that

MDP1 blocks degradation of DNA by DNases in vitro (unpublished observations), and this DNA-protective activity of MDP1 is one possible explanation.

Another possible explanation is the cell-binding activity of MDP1. To exert immunostimulatory activity, CpG DNA must attach to the macrophage surface and be internalized, with subsequent maturation of the phagosome (51). In our preliminary work, biotin-labeled ODN was more quickly bound to the macrophage surface and internalized when it was added with MDP1 (our unpublished observations). We have demonstrated that MDP1 binds to glycosaminoglycans and to A549 human lung epithelial cells through hyaluronic acid (16). After adding 0.5 μM MDP1, >95% of A549 cells became MDP1 positive in 60 min (16). In addition, it has been shown that HupB/MDP1 binds to C3 (52). Complement receptors are major receptors for *M. tuberculosis* on macrophages (53, 54). Collectively, it is reasonable to assume that MDP1 binds to macrophages through surface glycosaminoglycans or complement receptors. This cell-binding activity of MDP1 is advantageous for carrying DNA to/into macrophages, resulting in subsequent immunostimulation.

Immunization with MDP1 plus mycobacterial DNA significantly reduced the bacterial burden compared with treatment with Ag85B (Fig. 8). To develop effective vaccines against tuberculosis, additional studies are necessary to assess vaccine efficacy using MDP1 in conjunction with CpG-ODNs that can induce a Th1 response (32–34). Although the Ag85 complex has been widely studied as a major component of tuberculosis vaccines (11, 55), we did not observe a protective effect (Fig. 8). These conflicting results may be due to the mouse strains used in this experiment, because Ag85A and 85B induce protective immunity against mycobacterial infection in C57BL/6 mice (55, 56). The protective effect of Ag85B is conspicuous in guinea pigs as well (11). Guinea pigs are relatively susceptible to *M. tuberculosis* infection, whereas the mouse has low to moderate susceptibility (57, 58). In addition, guinea pigs, but not mice, develop cavitary lesions and caseous necrosis similar to human tuberculosis. It will be important to examine the protective effect of coadministration of MDP1 and DNA in a guinea pig model.

A key step in initiating adaptive immunity is the presentation of pathogen-derived peptides on class II MHC molecules by APCs. APC functions are up-regulated after recognition of pathogen-associated molecular patterns, including CpG DNA motifs (28). Therefore, we examined the effects of MDP1 on CpG ODN-mediated immune activation. We found that MDP1 magnified CpG-DNA effects, such as the production of the proinflammatory cytokines TNF-α and IL-6 (Fig. 9). As far as we know, MDP1 is the first protein identified that remarkably enhances CpG-mediated immune stimulation. Proinflammatory cytokines are critical for APC activation and promote the maturation of professional APCs. Immunostimulation induced by the interaction between MDP1 and CpG DNA might be involved in inducing strong adaptive immune responses against MDP1, which lead to protection (Fig. 8).

MyD88 is an adaptor molecule critical for the CpG-DNA-TLR9 signaling pathway (59, 60). Recently, it was shown that MyD88 KO mice are highly susceptible to *M. tuberculosis* (61) and *M. avium* (62), although mice with genetic mutations of TLR2 and TLR4 displayed comparable resistance as wild-type mice challenged with *M. tuberculosis* (63) and *M. avium* (62). These studies suggest that resistance to mycobacterial infection is regulated by multiple MyD88-dependent signals in addition to those attributed to TLR2 (64) or TLR4. As we show in this study, MDP1 stimulates TLR9-dependent immune responses by CpG ODN (Fig. 9), and the MDP1-DNA complex can induce protective immunity (Fig. 8). TLR9 signaling stimulated by MDP1-mycobacterial DNA complexes might be involved in MyD88-dependent antimycobacterial immunity.

The immunostimulatory activity of DNA was initially discovered in a DNA-rich fraction derived from BCG, referred to as MY1 (65, 66). Those studies demonstrated that the antitumor activity of MY1 was diminished by DNase treatment. MY1 is a mycobacterial nucleoid (65, 66). It is conceivable that MDP1 is involved in the activity of MY1.

The immunostimulatory activity of DNA has huge potential for immunotherapy against infectious, neoplastic, and allergic diseases (50, 67–69). To our knowledge, MDP1 is the first protein discovered that remarkably augments CpG-mediated immune stimulation (Fig. 9). MDP1 has great potential as an adjuvant for CpG-ODN-based immune interventions.

Acknowledgments

We are grateful to Drs. Naoya Ohara, Taisuke Tabira, and Sadamu Nagai for the gifts of purified proteins. We also thank Dr. Charles Scanga for prereading the manuscript, and Megumi Matsumoto and Sara Matsumoto for heartfelt encouragement.

Disclosures

The authors have no financial conflict of interest.

References

1. Wayne, L. G., and C. D. Sohaskey. 2001. Nonreplicating persistence of *Mycobacterium tuberculosis*. *Annu. Rev. Microbiol.* 55: 139–163.
2. Schwartzman, K. 2002. Latent tuberculosis infection: old problem, new priorities. *CMAJ* 166: 759–761.
3. Manabe, Y. C., and W. R. Bishai. 2000. Latent *Mycobacterium tuberculosis*-persistence, patience, and winning by waiting. *Nat. Med.* 6: 1327–1329.
4. Bloom, B. R. 2002. Tuberculosis: the global view. *N. Engl. J. Med.* 346: 1434–1435.
5. Horsburgh, C. R., Jr. 2004. Priorities for the treatment of latent tuberculosis infection in the United States. *N. Engl. J. Med.* 350: 2060–2067.
6. Colditz, G. A., T. F. Brewer, C. S. Berkey, M. E. Wilson, E. Burdick, H. V. Fineberg, and F. Mosteller. 1994. Efficacy of BCG vaccine in the prevention of tuberculosis: meta-analysis of the published literature. *J. Am. Med. Assoc.* 271: 698–702.
7. Collins, H. L., and S. H. Kaufmann. 2001. Prospects for better tuberculosis vaccines. *Lancet Infect. Dis.* 1: 21–28.
8. Roche, P. W., J. A. Triccas, and N. Winter. 1995. BCG vaccination against tuberculosis: past disappointments and future hopes. *Trends Microbiol.* 3: 397–401.
9. Milstien, J. B., and J. J. Gibson. 1990. Quality control of BCG vaccine by WHO: a review of factors that may influence vaccine effectiveness and safety. *Bull. World Health Organ.* 68: 93–108.
10. Sorensen, A. L., S. Nagai, G. Houen, P. Andersen, and A. B. Andersen. 1995. Purification and characterization of a low-molecular-mass T-cell antigen secreted by *Mycobacterium tuberculosis*. *Infect. Immun.* 63: 1710–1717.
11. Horwitz, M. A., B. W. Lee, B. J. Dillon, and G. Harth. 1995. Protective immunity against tuberculosis induced by vaccination with major extracellular proteins of *Mycobacterium tuberculosis*. *Proc. Natl. Acad. Sci. USA* 92: 1530–1534.
12. Skeiky, Y. A., M. R. Alderson, P. J. Ovendale, J. A. Guderian, L. Brandt, D. C. Dillon, A. Campos-Neto, Y. Lobet, W. Dalemans, I. M. Orme, et al. 2004. Differential immune responses and protective efficacy induced by components of a tuberculosis polyprotein vaccine, Mtb72F, delivered as naked DNA or recombinant protein. *J. Immunol.* 172: 7618–7628.
13. Tascon, R. E., M. J. Colston, S. Ragno, E. Stavropoulos, D. Gregory, and D. B. Lowrie. 1996. Vaccination against tuberculosis by DNA injection. *Nat. Med.* 2: 888–892.
14. Matsumoto, S., H. Yukitake, M. Furugen, T. Matsuo, T. Mineta, and T. Yamada. 1999. Identification of a novel DNA-binding protein from *Mycobacterium bovis* bacillus Calmette-Guérin. *Microbiol. Immunol.* 43: 1027–1036.
15. Furugen, M., S. Matsumoto, T. Matsuo, M. Matsumoto, and T. Yamada. 2001. Identification of the mycobacterial DNA-binding protein 1 region which suppresses transcription in vitro. *Microb. Pathog.* 30: 129–138.
16. Aoki, K., S. Matsumoto, Y. Hirayama, T. Wada, Y. Ozeki, M. Niki, P. Domenech, K. Umemori, S. Yamamoto, A. Mineda, et al. 2004. Extracellular mycobacterial DNA-binding protein 1 participates in *Mycobacterium*-lung epithelial cell interaction through hyaluronic acid. *J. Biol. Chem.* 279: 39798–39806.
17. Lee, B. H., B. Murugasu-Oei, and T. Dick. 1998. Upregulation of a histone-like protein in dormant *Mycobacterium smegmatis*. *Mol. Gen. Genet.* 260: 475–479.
18. Matsumoto, S., M. Furugen, H. Yukitake, and T. Yamada. 2000. The gene encoding mycobacterial DNA-binding protein 1 (MDP1) transformed rapidly growing bacteria to slowly growing bacteria. *FEMS Microbiol. Lett.* 182: 297–301.
19. Pethe, K., V. Puech, M. Daffe, C. Josenhans, H. Drobecq, C. Locht, and F. D. Menozzi. 2001. *Mycobacterium smegmatis* laminin-binding glycoprotein

shares epitopes with *Mycobacterium tuberculosis* heparin-binding haemagglutinin. *Mol. Microbiol.* 39: 89–99.
20. Shimoji, Y., V. Ng, K. Matsumura, V. A. Fischetti, and A. Rambukkana. 1999. A 21-kDa surface protein of *Mycobacterium leprae* binds peripheral nerve laminin-2 and mediates Schwann cell invasion. *Proc. Natl. Acad. Sci. USA* 96: 9857–9862.
21. Rambukkana, A., J. L. Salzer, P. D. Yurchenco, and E. I. Tuomanen. 1997. Neural targeting of *Mycobacterium leprae* mediated by the G domain of the laminin-α2 chain. *Cell* 88: 811–821.
22. Ng, V., G. Zanazzi, R. Timpl, J. F. Talts, J. L. Salzer, P. J. Brennan, and A. Rambukkana. 2000. Role of the cell wall phenolic glycolipid-1 in the peripheral nerve predilection of *Mycobacterium leprae*. *Cell* 103: 511–524.
23. Menozzi, F. D., J. H. Rouse, M. Alavi, M. Laude-Sharp, J. Muller, R. Bischoff, M. J. Brennan, and C. Locht. 1996. Identification of a heparin-binding hemagglutinin present in mycobacteria. *J. Exp. Med.* 184: 993–1001.
24. Hernandez-Pando, R., M. Jeyanathan, G. Mengistu, D. Aguilar, H. Orozco, M. Harboe, G. A. Rook, and G. Bjune. 2000. Persistence of DNA from *Mycobacterium tuberculosis* in superficially normal lung tissue during latent infection. *Lancet* 356: 2133–2138.
25. Prabhakar, S., P. S. Annapurna, N. K. Jain, A. B. Dey, J. S. Tyagi, and H. K. Prasad. 1998. Identification of an immunogenic histone-like protein (HLP*M*) of *Mycobacterium tuberculosis*. *Tuber. Lung Dis.* 79: 43–53.
26. Yamamoto, S., T. Yamamoto, T. Kataoka, E. Kuramoto, O. Yano, and T. Tokunaga. 1992. Unique palindromic sequences in synthetic oligonucleotides are required to induce IFN and augment IFN-mediated natural killer activity. *J. Immunol.* 148: 4072–4076.
27. Krieg, A. M., A. K. Yi, S. Matson, T. J. Waldschmidt, G. A. Bishop, R. Teasdale, G. A. Koretzky, and D. M. Klinman. 1995. CpG motifs in bacterial DNA trigger direct B-cell activation. *Nature* 374: 546–549.
28. Hemmi, H., O. Takeuchi, T. Kawai, T. Kaisho, S. Sato, H. Sanjo, M. Matsumoto, K. Hoshino, H. Wagner, K. Takeda, and S. Akira. 2000. A Toll-like receptor recognizes bacterial DNA. *Nature* 408: 740–745.
29. Nagai, S., H. G. Wiker, M. Harboe, and M. Kinomoto. 1991. Isolation and partial characterization of major protein antigens in the culture fluid of *Mycobacterium tuberculosis*. *Infect. Immun.* 59: 372–382.
30. Tabira, Y., N. Ohara, and T. Yamada. 2000. Identification and characterization of the ribosome-associated protein, HrpA, of bacillus Calmette-Guerin. *Microb. Pathog.* 29: 213–222.
31. Belisle J. T., and M. G. Sonnenberg. 1998. *Mycobacteria Protocol.* Humana Press, Totowa.
32. Gursel, I., M. Gursel, K. J. Ishii, and D. M. Klinman. 2001. Sterically stabilized cationic liposomes improve the uptake and immunostimulatory activity of CpG oligonucleotides. *J. Immunol.* 167: 3324–3328.
33. Davis, H. L., R. Weeratna, T. J. Waldschmidt, L. Tygrett, J. Schorr, A. M. Krieg, and R. Weeranta. 1998. CpG DNA is a potent enhancer of specific immunity in mice immunized with recombinant hepatitis B surface antigen. *J. Immunol.* 160: 870–876.
34. Walker, P. S., T. Scharton-Kersten, A. M. Krieg, L. Love-Homan, E. D. Rowton, M. C. Udey, and J. C. Vogel. 1999. Immunostimulatory oligodeoxynucleotides promote protective immunity and provide systemic therapy for leishmaniasis via IL-12- and IFN-γ-dependent mechanisms. *Proc. Natl. Acad. Sci. USA* 96: 6970–6975.
35. Pyles, R. B., D. Higgins, C. Chalk, A. Zalar, J. Eiden, C. Brown, G. Van Nest, and L. R. Stanberry. 2002. Use of immunostimulatory sequence-containing oligonucleotides as topical therapy for genital herpes simplex virus type 2 infection. *J. Virol.* 76: 11387–11396.
36. Klinman, D. M., J. Conover, and C. Coban. 1999. Repeated administration of synthetic oligodeoxynucleotides expressing CpG motifs provides long-term protection against bacterial infection. *Infect. Immun.* 67: 5658–5663.
37. Krieg, A. M., L. Love-Homan, A. K. Yi, and J. T. Harty. 1998. CpG DNA induces sustained IL-12 expression in vivo and resistance to *Listeria monocytogenes* challenge. *J. Immunol.* 161: 2428–2434.
38. Zimmermann, S., O. Egeter, S. Hausmann, G. B. Lipford, M. Rocken, H. Wagner, and K. Heeg. 1998. CpG oligodeoxynucleotides trigger protective and curative Th1 responses in lethal murine leishmaniasis. *J. Immunol.* 160: 3627–3630.
39. Ohara, N., M. Naito, C. Miyazaki, S. Matsumoto, Y. Tabira, and T. Yamada. 1997. HrpA, a new ribosome-associated protein which appears in heat-stressed *Mycobacterium bovis* bacillus Calmette-Guérin. *J. Bacteriol.* 179: 6495–6498.
40. Flynn, J. L., and J. Chan. 2001. Immunology of tuberculosis. *Annu. Rev. Immunol.* 19: 93–129.
41. Kaufmann, S. H. 2001. How can immunology contribute to the control of tuberculosis? *Nat. Rev. Immunol.* 1: 20–30.
42. Flynn, J. L., J. Chan, K. J. Triebold, D. K. Dalton, T. A. Stewart, and B. R. Bloom. 1993. An essential role for interferon γ in resistance to *Mycobacterium tuberculosis* infection. *J. Exp. Med.* 178: 2249–2254.
43. Cooper, A. M., D. K. Dalton, T. A. Stewart, J. P. Griffin, D. G. Russell, and I. M. Orme. 1993. Disseminated tuberculosis in interferon γ gene-disrupted mice. *J. Exp. Med.* 178: 2243–2247.
44. Coffman, R. L., B. W. Seymour, D. A. Lebman, D. D. Hiraki, J. A. Christiansen, B. Shrader, H. M. Cherwinski, H. F. Savelkoul, F. D. Finkelman, M. W. Bond, et al. 1988. The role of helper T cell products in mouse B cell differentiation and isotype regulation. *Immunol. Rev.* 102: 5–28.
45. Faquim-Mauro, E. L., R. L. Coffman, I. A. Abrahamsohn, and M. S. Macedo. 1999. Cutting edge: mouse IgG1 antibodies comprise two functionally distinct types that are differentially regulated by IL-4 and IL-12. *J. Immunol.* 163: 3572–3576.
46. Smith, K. M., L. Pottage, E. R. Thomas, A. J. Leishman, T. N. Doig, D. Xu, F. Y. Liew, and P. Garside. 2000. Th1 and Th2 CD4$^+$ T cells provide help for B cell clonal expansion and antibody synthesis in a similar manner in vivo. *J. Immunol.* 165: 3136–3144.
47. Poltorak, A., X. He, I. Smirnova, M. Y. Liu, C. Van Huffel, X. Du, D. Birdwell, E. Alejos, M. Silva, C. Galanos, et al. 1998. Defective LPS signaling in C3H/HeJ and C57BL/10ScCr mice: mutations in Tlr4 gene. *Science* 282: 2085–2088.
48. Qureshi, S. T., L. Lariviere, G. Leveque, S. Clermont, K. J. Moore, P. Gros, and D. Malo. 1999. Endotoxin-tolerant mice have mutations in Toll-like receptor 4 (Tlr4). *J. Exp. Med.* 189: 615–625.
49. Yamamoto, T., S. Yamamoto, T. Kataoka, and T. Tokunaga. 1994. Lipofection of synthetic oligodeoxyribonucleotide having a palindromic sequence of AACGTT to murine splenocytes enhances interferon production and natural killer activity. *Microbiol. Immunol.* 38: 831–836.
50. Krieg, A. M. 2002. CpG motifs in bacterial DNA and their immune effects. *Annu. Rev. Immunol.* 20: 709–760.
51. Hacker, H., H. Mischak, T. Miethke, S. Liptay, R. Schmid, T. Sparwasser, K. Heeg, G. B. Lipford, and H. Wagner. 1998. CpG-DNA-specific activation of antigen-presenting cells requires stress kinase activity and is preceded by non-specific endocytosis and endosomal maturation. *EMBO J.* 17: 6230–6240.
52. Mueller-Ortiz, S. L., E. Sepulveda, M. R. Olsen, C. Jagannath, A. R. Wanger, and S. J. Norris. 2002. Decreased infectivity despite unaltered C3 binding by a DeltahbhA mutant of *Mycobacterium tuberculosis*. *Infect. Immun.* 70: 6751–6760.
53. Hirsch, C. S., J. J. Ellner, D. G. Russell, and E. A. Rich. 1994. Complement receptor-mediated uptake and tumor necrosis factor-α-mediated growth inhibition of *Mycobacterium tuberculosis* by human alveolar macrophages. *J. Immunol.* 152: 743–753.
54. Schlesinger, L. S., C. G. Bellinger-Kawahara, N. R. Payne, and M. A. Horwitz. 1990. Phagocytosis of *Mycobacterium tuberculosis* is mediated by human monocyte complement receptors and complement component C3. *J. Immunol.* 144: 2771–2780.
55. Huygen, K., J. Content, O. Denis, D. L. Montgomery, A. M. Yawman, R. R. Deck, C. M. DeWitt, I. M. Orme, S. Baldwin, C. D'Souza, et al. 1996. Immunogenicity and protective efficacy of a tuberculosis DNA vaccine. *Nat. Med.* 2: 893–898.
56. Lozes, E., K. Huygen, J. Content, O. Denis, D. L. Montgomery, A. M. Yawman, P. Vandenbussche, J. P. Van Vooren, A. Drowart, J. B. Ulmer, et al. 1997. Immunogenicity and efficacy of a tuberculosis DNA vaccine encoding the components of the secreted antigen 85 complex. *Vaccine* 15: 830–833.
57. Riley, R. L., C. C. Mills, W. Nyka, N. Weinstock, P. B. Storey, L. U. Sultan, M. C. Riley, and W. F. Wells. 1959. Aerial dissemination of pulmonary tuberculosis: a two year study of contagion in a tuberculosis ward. *Am. J. Hyg.* 70: 185–196.
58. Smith, D. W., D. N. McMurray, E. H. Wiegeshaus, A. A. Grover, and G. E. Harding. 1970. Host-parasite relationships in experimental airborne tuberculosis. IV. Early events in the course of infection in vaccinated and nonvaccinated guinea pigs. *Am. Rev. Respir. Dis.* 102: 937–949.
59. Hacker, H., R. M. Vabulas, O. Takeuchi, K. Hoshino, S. Akira, and H. Wagner. 2000. Immune cell activation by bacterial CpG-DNA through myeloid differentiation marker 88 and tumor necrosis factor receptor-associated factor (TRAF)6. *J. Exp. Med.* 192: 595–600.
60. Schnare, M., A. C. Holt, K. Takeda, S. Akira, and R. Medzhitov. 2000. Recognition of CpG DNA is mediated by signaling pathways dependent on the adaptor protein MyD88. *Curr. Biol.* 10: 1139–1142.
61. Scanga, C. A., A. Bafica, C. G. Feng, A. W. Cheever, S. Hieny, and A. Sher. 2004. MyD88-deficient mice display a profound loss in resistance to *Mycobacterium tuberculosis* associated with partially impaired Th1 cytokine and nitric oxide synthase 2 expression. *Infect. Immun.* 72: 2400–2404.
62. Feng, C. G., C. A. Scanga, C. M. Collazo-Custodio, A. W. Cheever, S. Hieny, P. Caspar, and A. Sher. 2003. Mice lacking myeloid differentiation factor 88 display profound defects in host resistance and immune responses to *Mycobacterium avium* infection not exhibited by Toll-like receptor 2 (TLR2)- and TLR4-deficient animals. *J. Immunol.* 171: 4758–4764.
63. Reiling, N., C. Holscher, A. Fehrenbach, S. Kroger, C. J. Kirschning, S. Goyert, and S. Ehlers. 2002. Cutting edge: Toll-like receptor (TLR)2- and TLR4-mediated pathogen recognition in resistance to airborne infection with *Mycobacterium tuberculosis*. *J. Immunol.* 169: 3480–3484.
64. Thoma-Uszynski, S., S. Stenger, O. Takeuchi, M. T. Ochoa, M. Engele, P. A. Sieling, P. F. Barnes, M. Rollinghoff, P. L. Bolcskei, M. Wagner, et al. 2001. Induction of direct antimicrobial activity through mammalian Toll-like receptors. *Science* 291: 1544–1547.
65. Tokunaga, T., H. Yamamoto, S. Shimada, H. Abe, T. Fukuda, Y. Fujisawa, Y. Furutani, O. Yano, T. Kataoka, T. Sudo, et al. 1984. Antitumor activity of deoxyribonucleic acid fraction from *Mycobacterium bovis* BCG. I. Isolation, physicochemical characterization, and antitumor activity. *J. Natl. Cancer Inst.* 72: 955–962.
66. Shimada, S., O. Yano, H. Inoue, E. Kuramoto, T. Fukuda, H. Yamamoto, T. Kataoka, and T. Tokunaga. 1985. Antitumor activity of the DNA fraction from *Mycobacterium bovis* BCG. II. Effects on various syngeneic mouse tumors. *J. Natl. Cancer Inst.* 74: 681–688.
67. Halperin, S. A., G. Van Nest, B. Smith, S. Abtahi, H. Whiley, and J. J. Eiden. 2003. A phase I study of the safety and immunogenicity of recombinant hepatitis B surface antigen co-administered with an immunostimulatory phosphorothioate oligonucleotide adjuvant. *Vaccine* 21: 2461–2467.
68. Jahrsdorfer, B., and G. J. Weiner. 2003. CpG oligodeoxynucleotides for immune stimulation in cancer immunotherapy. *Curr. Opin. Investig. Drugs.* 4: 686–690.
69. Klinman, D. M. 2004. Immunotherapeutic uses of CpG oligodeoxynucleotides. *Nat. Rev. Immunol.* 4: 249–258.

12

Development of HVJ Envelope Vector and Its Application to Gene Therapy

Yasufumi Kaneda,* Seiji Yamamoto,* and Toshihiro Nakajima†

*Division of Gene Therapy Science, Graduate School of Medicine
Osaka University, Suita, Osaka 565-0871, Japan
†GenomIdea Inc., 7-7-15 Saito-Asagi, Ibaragi
Osaka 567-0085, Japan

Advances in Genetics, Vol. 53

0065-2660/05 $35.00
DOI: 10.1016/S0065-2660(05)53012-8

ABSTRACT

To create a highly efficient vector system that is minimally invasive, we initially developed liposomes that contained fusion proteins from the hemagglutinating virus of Japan (HVJ; Sendai virus). These HVJ-liposomes delivered genes and drugs to cultured cells and tissues. To simplify the vector system and develop more efficient vectors, the next approach was to convert viruses to non-viral vectors. Based on this concept, we recently developed the HVJ envelope vector. HVJ with robust fusion activity was inactivated, and exogenous DNA was incorporated into the viral envelope by detergent treatment and centrifugation. The resulting HVJ envelope vector introduced plasmid DNA efficiently and rapidly into both cultured cells *in vitro* and organs *in vivo*. Furthermore, proteins, synthetic oligonucleotides, and drugs have also been effectively introduced into cells using the HVJ envelope vector. The HVJ envelope vector is a promising tool for both *ex vivo* and *in vivo* gene therapy experiments. Hearing impairment in rats was prevented and treated by hepatocyte growth factor gene transfer to cerebrospinal fluid using HVJ envelope vector. For cancer treatment, tumor-associated antigen genes were delivered efficiently to mouse dendritic cells to evoke an anti-cancer immune response. HVJ envelope vector fused dendritic cells and tumor cells and simultaneously delivered cytokine genes, such as IL-12, to the hybrid cells. This strategy successfully prevented and treated cancers in mice by stimulating the presentation of tumor antigens and the maturation of T cells. For human gene therapy, a pilot plant to commercially produce clinical grade HVJ envelope vector has been established.

I. INTRODUCTION

Gene therapy is a promising treatment for intractable human diseases (Cavazzana-Calvo *et al.*, 2004; Marshall, 1995), but further development of effective gene transfer vector systems is required for the advancement of human gene therapy (Mulligan, 1993). Efficient and minimally invasive vector systems appear to be most appropriate for gene therapy. Numerous viral and non-viral (synthetic) methods for gene transfer have been developed (Lam and Brakefield, 2000; Ledley, 1995; Li and Huang, 2000; Mulligan, 1993). Viral methods are generally more efficient than non-viral methods for the delivery of genes to cells, but the safety of viral vectors is of concern due to the concomitant introduction of genetic elements from parent viruses, leaky expression of viral genes, immunogenicity, and changes in the host genome structure (Mulligan, 1995) as pointed out in the SCID-X1 gene therapy clinical trial (Cavazzana-Calvo *et al.*, 2004). Because non-viral vectors are less toxic and less immunogenic than viral vectors,

the development of non-viral vectors has been pursued. Various modifications have been made to enhance the efficiency of gene delivery by non-viral vectors. Liposomes have been used to target and introduce macromolecules into cells. However, the gene transfer efficiency of liposomes was low and varied during the early days of liposome development. The synthesis of cationic lipids produced a revolutionary improvement in gene transfer efficiency by Felgner *et al.* (1987). They also developed a new type of liposome-DNA complex called a "lipoplex." Prior to this development, DNA had been incorporated into liposomes, but, with lipoplex, an electrostatic complex was made between negatively charged DNA and positively charged cationic liposomes. Numerous cationic lipids have been synthesized to further improve transfection efficiency and reduce the cytotoxicity of lipoplex (Li and Huang, 2000). Nevertheless, in lipoplex-mediated transfection, DNA is still delivered into cells by phagocytosis or endocytosis, not by fusion.

Because molecules that enter the cell by phagocytosis or endocytosis often become degraded before reaching the cytoplasm, fusion-mediated delivery systems have been developed. A fusigenic viral liposome with fusion proteins derived from hemagglutinating virus of Japan (HVJ; Sendai virus) was constructed (Kaneda *et al.*, 1999). HVJ fuses with the cell membrane at a neutral pH, and the hemagglutinin-neuraminidase (HN) protein and fusion (F) protein of the virus contribute to cell fusion (Okada, 1993). For fusion-mediated gene transfer, DNA-loaded liposomes were fused with UV-inactivated HVJ to form the fusigenic viral-liposome called HVJ-liposome.

Fusion-mediated delivery protected the molecules in the endosomes and lysosomes from degradation (Dzau *et al.*, 1996). When fluorescein isothiocyanate (FITC)-tagged oligodeoxynucleotide (ODN) was introduced into vascular smooth muscle cells using HVJ-liposomes, fluorescence was detected in the nuclei 5 min after transfer, and fluorescence was stable in the nucleus for at least 72 h In contrast, fluorescence was observed in cellular components (most likely, endosomes) and not in the nucleus when FITC-ODN was transferred directly in the absence of HVJ-liposomes, and no fluorescence was detected 24 h after transfer. Using a fluorescence resonance energy transfer system, we demonstrated that more than 80% of oligonucleotides labeled with two different fluorescent dyes at the 5′ and 3′ ends were intact in the nucleus, while less than 30% of the oligonucleotides were intact when Lipofectin was used. (Nakamura *et al.*, 2001).

Another advantage of HVJ-liposomes is the ability to perform repeated injections. Gene transfer to rat liver cells was not inhibited by repeated injections. After repeated injections, the anti-HVJ antibodies generated in the rat were not sufficient to neutralize HVJ-liposomes. Cytotoxic T cells recognizing HVJ determinants were not detected in the rats transfected repeatedly with HVJ-liposomes (Hirano *et al.*, 1998).